REVIEW ARTICLE

Electric probes for plasmas: The link between theory and instrument

V. I. Demidov, S. V. Ratynskaia, and K. Rypdal
Department of Physics, University of Tromsø, 9037 Tromsø, Norway

(Received 18 May 2001; accepted for publication 7 July 2002)

Electric probe methods for diagnostics of plasmas are reviewed with emphasis on the link between the appropriate probe theories and the instrumental design. The starting point is an elementary discussion of the working principles and a discussion of the physical quantities that can be measured by the probe method. This is followed by a systematic classification of the various regimes of probe operation and a summary of theories and methods for measurements of charged particle distributions. Application of a single probe and probe clusters for measurements of fluid observables is discussed. Probe clusters permit both instantaneous and time-averaged measurements without sweeping the probe voltage. Two classes of applications are presented as illustrations of the methods reviewed. These are measurements of cross sections and collision frequencies (plasma electron spectroscopy), and measurements of fluctuations and anomalous transport in magnetized plasma. [DOI: 10.1063/1.1505099]

I. INTRODUCTION

A plasma is a fully or partially ionized gas with practically equal densities of positive and negative charged particles.[1] Diagnostics of plasmas fall roughly into three categories: passive remote sensing, active noncontact methods, and contact methods. Passive sensing of incoming radiation is all that is available for plasma astrophysics studying the Sun or plasma phenomena related to objects beyond the Solar system. Active noncontact methods are widely applied to geophysical plasmas such as the ionosphere (radar scattering) and to hot laboratory plasmas (scattering of electromagnetic radiation or particle beams). Contact methods are applied to interplanetary, magnetospheric and ionospheric plasmas, and to cold laboratory plasmas. Among the contact methods, electric probes are without doubt the most widely used. Some of the techniques reviewed here can be applied to *in situ* experiments in space plasmas, but the context in which they are discussed is limited to laboratory plasmas.

Basically, the electric probe is a conducting object inserted into the plasma, and connected to the outside world through some kind of electrical circuitry. Two requirements need to be fulfilled in order to operate a probe successfully. First, the probe must be able to withstand the heat load from the plasma without being severely damaged. This excludes the application of probes in the core of most magnetic confinement devices, and requires quite robust probe constructions in intermediate dense and hot plasmas, such as in the edge of such devices. Second, the probe should not perturb the global state of the plasma, and this calls for a small probing object compared with typical plasma scale lengths.

The subject of electric probes in plasmas is huge and thousands of references on the subject can be found in the literature. It is, therefore, necessary to limit the scope of any review on this subject. We limit the class of plasmas to those sufficiently cold that very small probes can survive for the time required to perform the desired measurement. We also do not include measurement situations where the proximity of a nearby wall or large material object has to be taken into account. This excludes flush mounted probes and probe arrays mounted on large surfaces facing the plasma. We also exclude plasmas that require a theoretical framework for interpretation of probe data which goes beyond what is described in Sec. II of this article. This means that we will not discuss probes for chemically reactive and dusty plasmas, or for strongly magnetized, fully ionized plasma, which require modeling of viscous or anomalous transport processes for the calculation of the probe current. The latter excludes from this review standard probe measurements in magnetic confinement plasmas, because under these conditions the ion Larmor radius is smaller than the probe dimension, and the proper modeling of the ion transport remains a controversial issue which we have chosen not to deal with in this review. However, the review includes weakly magnetized plasma, in the sense that the electron (but not ion) Larmor radius is smaller than the probe dimension. We will also deal with strongly magnetized, weakly ionized plasma, since in this case the ion transport is dominated by ion-neutral collisions, which can easily be modeled even for magnetized ions. This means that we include measurements in a large class of magnetized plasma devices constructed for plasma processing, basic plasma physics, and study of low frequency fluctuations and anomalous transport in the edge of magnetic confinement plasmas.

Within our scope we will not consider all existing probe models but rather give basic ideas and provide corresponding references. It should also be emphasized that only a selection of probe constructions and configurations of probe clusters

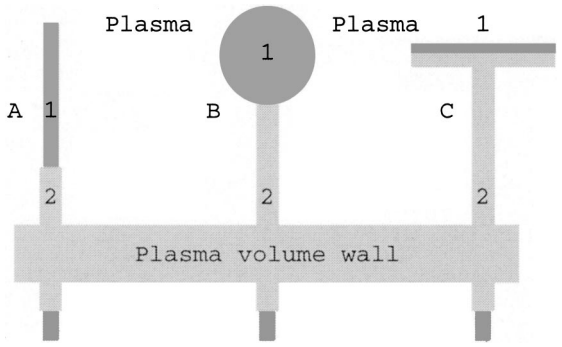

FIG. 1. Typical probe constructions. Cylindrical (A), spherical (B), and flat (C) probes. Conductor (1) and insulator (2).

found in the literature is described, focusing on a few applications. However, the probe constructions, as well as the applications, are carefully selected to illustrate the power and limitations of electric probe techniques.

A. Basic principles of probe operation

Electric probes were first applied to plasmas by Langmuir and collaborators.[2,3] The operating principle is very simple. An external electrical circuit allows variation of the probe voltage V with respect to the plasma and to measure the current–voltage characteristic $I(V)$. It is also possible to measure the floating probe voltage V_f. In this case the probe is connected to ground through a very high resistance, so that I is practically zero.

A probe theory creates a connection between the measured probe currents and/or voltages and parameters of the undisturbed plasma. Unfortunately, the simplicity of the operating scheme is not reflected by the appropriate theories for most plasma regimes. Thus, the main purpose of this review is to serve as a guide to find the appropriate theory for a given set of experimental conditions and the optimal probe design.

Electric probes come in all sizes and shapes, but the most common shapes are spheres, cylinders, and flat disks (see Fig. 1). They are usually made out of materials like molybdenum, tungsten, graphite and, for chemically active plasmas, platinum and gold. The probe holder can be made from glass, quartz, or ceramic materials.

A simple probe circuit is presented in Fig. 2. The probe (1) is given a voltage V_r with respect to a reference electrode (2). An anode may be taken as the reference electrode (in discharge plasmas the voltage between the anode and the plasma is usually less than the voltage between the cathode and the plasma). Often the reference electrode is the grounded vessel wall. In electrode-free plasmas or in a double-probe method another probe may be taken as the reference electrode.

A typical $I-V$ characteristic of the probe is presented in Fig. 3. It can be divided into three distinct parts. For sufficiently negative probe voltage ($V<V_a$) the probe collects mainly positive ions, and the corresponding current is called the ion saturation current $I_i^{\rm sat}$. If $V_a<V<V_b$ (the transition part of the characteristic) the probe collects ions and electrons, and for $V=V_f$, ion I_i and electron I_e currents are equal. For V equal to the plasma potential V_p the characteristic may exhibit a ''knee'' because the potential changes character from attracting ions and repelling electrons to repelling ions and attracting electrons. For positive voltage $V>V_b$ the probe only collects electrons (the electron saturation current $I_e^{\rm sat}$. In this article we use the convention of plotting current *to* the probe. Many recent authors have adopted this convention but up till the 1980s the opposite convention of plotting current *from* the probe was almost universally used.

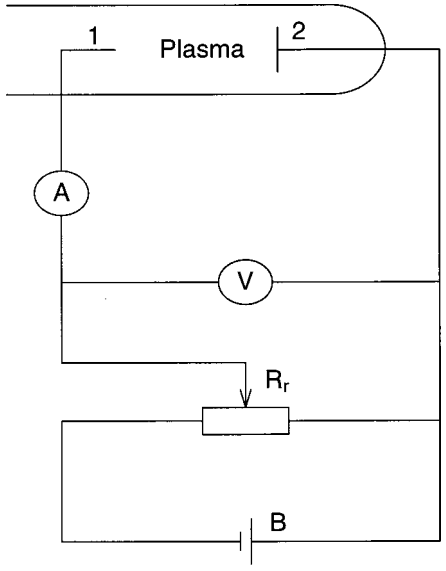

FIG. 2. Probe measurement circuit. Probe (1), reference electrode (2), voltage source (B), resistor (R_r).

The probe $I-V$ characteristic contains information about fluid observables as well as more detailed information about energy distributions of electrons and ions. One can extract densities of electrons n_e, positive n_a^+, and negative n_a^- ions, temperatures (average energies) of electrons T_e and ions T_i, average frequencies of plasma particle collisions $\overline{\nu}$, and for

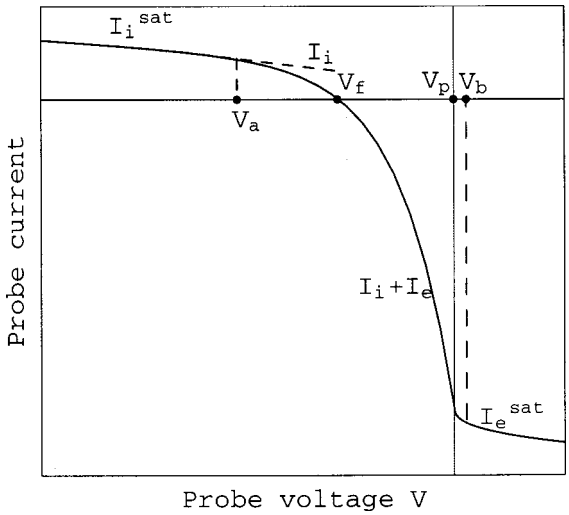

FIG. 3. General form of the probe characteristic. V_f is the floating probe potential, $V_p=0$ is the plasma potential, I_e, $I_e^{\rm sat}$, I_i, and $I_i^{\rm sat}$ are the electron, electron saturation, ion, and ion saturation currents, respectively. For $V<V_a$ the probe collects the ion saturation current and for $V>V_b$ it collects the electron saturation current.

particular probe constructions plasma flow velocities. T_e and T_i can be extracted from the transition part of the characteristic and the other quantities basically from the saturation currents. The transition part of the characteristic can also provide the plasma potential V_p. Measurement of V_p by two probes yields one spatial component of the electric field. Measurements of these fluid observables allow us to calculate other important parameters, for instance anomalous cross-field particle fluxes in a magnetized plasmas.

Electron (EDF) and ion (IDF) velocity (energy) distribution functions may be extracted only from the transition part of the $I-V$ characteristic. This part contains information about the energy dependence of plasma particle collision frequencies ν, and reflection coefficients of electrons from plasma boundaries (surfaces of the probe and plasma container) (see, for instance, Sec. V A).

Thus, the $I-V$ probe characteristic allows us, in principle, to find most of the parameters for fluid or kinetic description of the plasma. However, the practical feasibility of extracting undisturbed plasma parameters depends strongly on the plasma conditions and the probe construction. As a rule, it is possible to extract electron density n_e, temperature (average energy) T_e, and plasma potential V_p for a wide range of plasma conditions. Electron energy distributions can be measured for gas pressures up to 10^4 Pa and magnetic fields up to a few tenths of T (see Sec. III A). Ion energy distributions, T_i and other parameters, however, can only be measured in special cases.

Even though the electric probe method is as old as plasma physics itself, the potential of the method has not yet been fully exploited. New probe theories and constructions constantly appear and the results have been summarized in numerous reviews and monographs.[4–25] In spite of this, incorrect applications of electric probes are commonly found in the literature. The errors mainly arise from lack of awareness about the multitude of regimes of probe operation and the limits of validity of theories. The purpose of the present review is mainly to give a systematic overview of these regimes and to demonstrate how this can be implemented in a broad range of probe designs and applications.

B. Outline of review

Section II contains a discussion of the assumptions underlying the various probe theories, and of the validity of the numerous idealizations made in interpreting probe data. Section III deals with the most detailed information that can be obtained by electric probes, the charged particle energy distribution functions. Section IV treats spatially localized measurements of instantaneous or time-averaged fluid variables, which have the advantage of being directly comparable with results obtained from theoretical fluid descriptions of the plasma equilibrium or of plasma fluctuations and turbulence. In Sec. V we describe two groups of applications, each illustrating the usefulness of the measurements described in Secs. III and IV. The various probe designs are described in the section where they first are discussed. Section VI contains some rather philosophical remarks which puts the subject of the review in a wider context. The reader, who during the study of a particular part of the article feels bewildered by the huge zoo of operating regimes and probe designs, should consult this section to regain the motivation to read further.

II. BASIC CONSIDERATIONS

A. Classification of probe operation regimes

In Sec. I it was stressed that data from electric probe measurements usually are of little value without a proper theory for the $I-V$ probe characteristic. The theory is based on the fact that the plasma shields any charged object,[1,26] and hence the perturbed plasma region is confined to the close vicinity of the probe. Thus, the $I-V$ characteristic contains information about the unperturbed plasma bordering this perturbed volume. By extracting this information one can obtain the local parameters of the undisturbed plasma with spatial resolution defined by the size of the disturbed region.

In its most fundamental form the probe problem consists of two distinct parts. First, the density and the velocity distributions of the charged particle species are assumed to be known, and one attempts to calculate the $I-V$ characteristic by solving the equations of motion of all charged particles traversing the perturbed region. This requires knowledge about the self-consistent potential profile throughout the disturbed region. Second, the inverse problem has to be solved, i.e., densities and distribution functions should be derived from the $I-V$ characteristic. There are many works devoted to this very complicated problem (see, for example, Refs. 9 and 10), where the calculations have been made for some particular cases.

However, the problem can be simplified for many cases of interest by dividing the region disturbed by the probe into a (nonquasineutral) sheath and quasineutral plasma (presheath).[5–10] In the sheath the electron and ion densities are significantly different and it appears only if the potential difference V between probe and plasma is so large that a significant fraction of the particles of the repelled species never reaches the probe. As a rule of the thumb this is the case if $|V|>\frac{1}{2}T/e$, where T is the temperature of the repelled particles and e is the proton charge ($+1.6\times10^{-19}$ C). This is the Bohm sheath criterion.[1,4] With this simplification the self-consistent problem may be solved for the sheath and presheath separately and the solutions are connected at the interface between the two regions. The resulting probe characteristic depends on a set of parameters, which can be naturally obtained from the equations describing plasma and sheath.[10]

A completely general theory describing the collection of charged particles by a probe does not exist. The appropriate theory depends on the parameters of the plasma and the size and shape of the probe. In an unmagnetized plasma the following parameters constitute the basis of probe theories:

1. Mean-free-path of electrons, λ_e and ions, λ_i

The electron mean-free-path λ_e is the average distance between collisions defined by

$$\lambda_e(v)=v\,\tau_e(v)=\frac{v}{\nu_e(v)}=\frac{1}{ns_e(v)}, \tag{1}$$

where $\tau_e(v)$ is the average intercollisional time, ν_e is the frequency of electron collisions with neutrals and electrons, $s_e(v)$ is the momentum transfer scattering cross section for electrons, n is the density of the colliding particle species (ions, neutrals or electrons) and v is the velocity of the electron. For ions, the subscript e should be replaced by i. During one collision the particle loses its directed velocity, so the mean-free path is sometimes called momentum or directed velocity relaxation length.

For calculations of λ_e and λ_i, corresponding cross sections can be taken, for instance, from Refs. 27–32. For estimation of the elastic electron-atomic collision frequency in noble gases the expression

$$\nu_a(\varepsilon)=\nu_0 p(\varepsilon/\varepsilon_1)^{\gamma} \tag{2}$$

can be used.[33] Here, ν_a is in s^{-1}, p is a gas pressure in Pa, and ε is the electron energy in eV. For He $\gamma=0$, $\nu_0=1.88\times10^7\,s^{-1}\,Pa^{-1}$, $\varepsilon_1=21.2$ eV; for Ne $\gamma=1$, $\nu_0=2.1\times10^7\,s^{-1}\,Pa^{-1}$, $\varepsilon_1=16.7$ eV; for Ar $\gamma=3$, $\nu_0=1.28\times10^8\,s^{-1}\,Pa^{-1}$, $\varepsilon_1=11.2$ eV. The frequency of collisions of an electron with energy ε with other electrons which have Maxwellian distribution and temperature T_e is

$$\nu_{ee}(\varepsilon)=1.54\times10^{-11}\frac{n_e}{\varepsilon^{3/2}}\ln\left[5.17\times10^{12}\varepsilon\sqrt{\frac{T_e}{n_e}}\right], \tag{3}$$

where ν_{ee} is in s^{-1}, n_e is the density of electrons in m^{-3}, T_e and ε in eV.[26]

2. Electron energy relaxation length, λ_ε

Let t_ε be the time an electron needs to lose its energy in collisional processes (energy relaxation time). If electron-electron collisions are dominant, this requires only one collision, and the energy relaxation length corresponds to the mean-free path. If elastic collisions with heavy particles of mass m_a dominate, a large number of collisions ($\sim1/\delta$, where $\delta=2m_e/m_a$, and m_e is the electron mass) are required for energy relaxation, and the characteristic length a particle diffuses during the time t_ε is the energy relaxation length,[34]

$$\lambda_\varepsilon=2\sqrt{D_e t_\varepsilon}, \tag{4}$$

where $D_e=\lambda_e v/3$ is the electron diffusion coefficient. If the electrons lose their energies due to electron–electron collisions and elastic and inelastic electron-atomic collisions, then[21,35]

$$\lambda_\varepsilon\approx2\sqrt{D_e}(\nu_{ee}+\delta\nu_a+\nu^*)^{-0.5}, \tag{5}$$

where ν^* is the inelastic electron-atomic collision frequency.

For the case of atomic gases and weakly ionized plasma, where the condition ν_e, $\nu^*\ll\nu_a$ is satisfied (i.e., the electron loses its energy mostly due to electron-atomic elastic collisions), we have $\lambda_\varepsilon\approx\lambda_e/\sqrt{\delta}\sim100\lambda_e$. It means that for electrons energy relaxation is much slower than momentum relaxation, and it occurs on a much larger length scale $\lambda_\varepsilon\gg\lambda_e$. Note that for ions the energy relaxation length is equal to the mean-free path. The energy relaxation length is the basis of the nonlocal approach that will be discussed at the end of this subsection.

3. Characteristic probe dimension, d

This is a length (sometimes called the diffusion length) which depends on the size and geometry of the probe. If compared with the mean-free-path this parameter allows us to distinguish collisionless ($d\ll\lambda_{e,i}$) and diffusive ($d\gg\lambda_{e,i}$) regimes. The diffusion length can be calculated by applying methods developed for solving the diffusion equation.[36] The stationary problem reduces to the Laplace equation (if the plasma is unmagnetized), which explains why the solution depends only on geometry, and not on the specific diffusion coefficient. The diffusion length is a characteristic length for the decay of this solution. For instance, $d\approx R$ for a spherical, $d\approx R\ln[\pi L/(4R)]$ for a cylindrical, and $d\approx\pi R/4$ for a disk probe, respectively. Here, R is the probe radius and L is the length of the cylindrical probe.

4. Sheath thickness, h

In the literature one can find various calculations of the sheath thickness.[5,6,9,10,37–39] The fundamental parameter is the Debye length[26]

$$R_D=\frac{1}{\sqrt{4\pi n_e e^2}}\left(\frac{T_e T_i}{T_e+T_i}\right)^{1/2}, \tag{6}$$

but in general h can be much larger than R_D. The thickness of a collisionless plane sheath can be estimated as[40]

$$h\approx R_D\left(\frac{e|V|}{T_e}\right)^{3/4} \tag{7}$$

and if $e|V|\gg T_e$ then $h\gg R_D$. The same formula can be used for calculation of h for a thin (compared to the probe dimension) nonplane sheath. Calculations of h for a thick collisionless sheath in a plasma with a non-Maxwellian EDF is given, for instance, in Ref. 39.

In practice, it is more convenient to express the sheath thickness via directly measured quantities such as the probe current and probe voltage. Thus, for $|\mathrm{eV}|\gg T_e/e$ Eq. (7) can be rewritten as

$$h_{e,i}=\left(\frac{2}{e m_{e,i}}\right)^{1/4}\frac{V^{3/4}}{3\sqrt{\pi}j_{e,i}}, \tag{8}$$

where $h_{i,e}$ is the electron (positive probe voltage) and ion (negative probe voltage) sheath thickness, respectively. Here, m_i is the ion mass and $j_{e,i}$ are the electron and ion current density.

The thickness of a collisional electron or ion sheath for a cylindrical probe can be calculated as[41]

$$h_{e,i}=0.0013R\left(\frac{\lambda_{e,i}LV^2}{\sqrt{T_{e,i}m_{e,i}}R^2I_{e,i}}\right)^{0.33}. \tag{9}$$

Here V is in V, I is in A, $m_{e,i}$ is in amu, and $T_{e,i}$ is in eV.

For $eE\lambda_i>T_i$ ions have anomalous drift inside the sheath, i.e., the ion drift velocity is proportional to $\sqrt{E}$, where E is electric field. In this case, radius $\rho_i=R+h_i$ of a collisional ion sheath for a cylindrical probe is given as[37]

TABLE I. The main regimes for electrons in a weakly ionized unmagnetized plasma. For a magnetized plasma, parallel or perpendicular parameters should be compared, respectively.

	Regime	Subregime
I	Collisionless $\lambda_e \gg d+h$	(a) Orbital limited thick sheath $\lambda_\varepsilon \gg \lambda_e \gg h \gg d$
		(b) Conventional thin sheath $\lambda_\varepsilon \gg \lambda_e \gg d \gg h$
II	Nonlocal $\lambda_\varepsilon \gg d+h \gg \lambda_e$	(a) Collisional thick sheath $\lambda_\varepsilon \gg h \gg \lambda_e \gg d$
		(b) Collisional thick sheath (large probe) $\lambda_\varepsilon \gg h \gg d \gg \lambda_e$
		(c) Collisional thin sheath $\lambda_\varepsilon \gg d \gg h \gg \lambda_e$
		(d) Collisionless thin sheath $\lambda_\varepsilon \gg d \gg \lambda_e \gg h$
III	Hydrodynamic (local) $d+h \gg \lambda_\varepsilon$	(a) Collisional thick sheath (small probe) $h \gg \lambda_\varepsilon \gg \lambda_e \gg d$
		(b) Collisional thick sheath (diffusive probe) $h \gg \lambda_\varepsilon \gg d \gg \lambda_e$
		(c) Collisional thick sheath $h \gg d \gg \lambda_\varepsilon \gg \lambda_e$
		(d) Collisional thin sheath $d \gg h \gg \lambda_\varepsilon \gg \lambda_e$
		(e) Collisional thin sheath (large probe) $d \gg \lambda_\varepsilon \gg h \gg \lambda_e$
		(f) Collisionless thin sheath $d \gg \lambda_\varepsilon \gg \lambda_e \gg h$

$$\rho_i = R(1+q)(1+0.05q); \quad q = \frac{9.2\times 10^{-4}}{R}\left(\frac{|V|^3 \lambda_i}{j_i^2 m_i}\right)^{1/5}. \tag{10}$$

Here V is in V, j_i is in A/m^2, λ_i and R are in m, and m_i is in amu.

The presence of a magnetic field introduces anisotropy in the plasma making the theoretical description of probes more complicated. In a magnetized plasma electron, R_{Le} and ion, R_{Li} Larmor radii are important. It should be taken into account that the above parameters are different parallel and perpendicular to the field. Define $\eta_{e,i} = \sqrt{1+x_{e,i}^2}$ and $x_{e,i} = \lambda_{e,i}/R_{\mathrm{Le,Li}}$. Then we have $\lambda_{e,i\parallel} = \lambda_{e,i}$, $\lambda_{\varepsilon\parallel} = \lambda_\varepsilon$, $\lambda_{e,i\perp} = \lambda_{e,i}/\eta_{e,i}$, $\lambda_{\varepsilon\perp} = \lambda_\varepsilon/\eta_e$,[42,43] and $d_{e,i\perp} = d_{e,i\parallel}/\eta_{e,i}$. In this case the characteristic probe dimension (diffusion length) $d_{e,i\perp}$ depends not only on probe geometry, but also on certain plasma parameters and the probe orientation with respect to the magnetic field. Since all lengths are multiplied by the factor $\eta_{e,i}$ when comparing parallel and perpendicular lengths, we can use either parallel or perpendicular lengths when defining different probe operation regimes for magnetized plasmas (see Table I). In general, the modeling of the sheath structure in the presence of a magnetic field is a complicated task.[44]

With respect to the parameters listed above, it is possible to indicate a set of asymptotic regimes of probe operation where the construction of an analytical model for the probe characteristic is more feasible. It is desirable to conduct measurements in one of these asymptotic regimes and sometimes it can be done by choosing appropriate probe shape, size, and (in magnetized plasma) orientation. The essence of the following classification scheme is taken from Refs. 10 and 21.

In the absence of magnetic field, the main regimes for electron probe current in a weakly ionized plasma may be presented as in Table I.

For electrons in a fully ionized plasma, and for ions, regime II (nonlocal) does not exist. In this case there are regimes I ($\lambda_{e,i} \gg h \gg d$, and $\lambda_{e,i} \gg d \gg h$) and III ($h \gg \lambda_{e,i} \gg d$, $h \gg d \gg \lambda_{e,i}$, $d \gg h \gg \lambda_{e,i}$, and $d \gg \lambda_{e,i} \gg h$) only. Note, that the electrons and ions can be in different regimes at the same plasma conditions, as $\lambda_e \neq \lambda_i$. They can also be in different regimes depending on the probe voltage, because the sheath thickness h depends on both magnitude and sign of probe voltage. As discussed above, in the case of a magnetized plasma the above classifications are valid if we compare either perpendicular or parallel lengths.

For more complicated plasmas (flowing, turbulent, chemically active, etc.) other characteristic lengths λ_x have to be introduced. For instance, a characteristic length of ionization or recombination for ions can be defined as[21]

$$\lambda_{\mathrm{ch}} = \left[D_i \left(1 + \frac{T_e}{T_i} \right) \tau_{\mathrm{ch}} \right]^{0.5},$$

where D_i is the ion diffusion coefficient and τ_{ch} is a characteristic time of the reaction. For ionization $\tau_{\mathrm{ch}} = (n_a \beta_i)^{-1}$ (β_i is the coefficient of ionization, n_a is density of neutrals), for recombination $\tau_{\mathrm{ch}} = (n_e \beta_r)^{-1}$ (β_r is the coefficient of recombination). In the presence of plasma turbulence, the characteristic length of fluctuation λ_{fl} can be defined as $\lambda_{\mathrm{tur}}/(2\pi)$, where λ_{tur} is the turbulent wave length. Then, if $\lambda_x \gg d+h$, the influence of these processes on the probe current can be neglected although the global plasma properties can be determined by them. In the opposite case the current collection can be governed by turbulence, chemical reactions, etc., which is beyond the scope of this review.

In practice, however, it is not always possible to calculate or measure λ_x. In some cases it is possible to test experimentally whether the current collection is governed by such mechanisms. Examples of some methods are mentioned at the end of Sec. IV C.

As an illustration, we estimate the essential plasma parameters for a weakly ionized neon plasma and indicate the appropriate probe operation regimes.[21] In this case $\lambda_e = 0.17/p$, $\lambda_i = 0.006/p$, $\lambda_\varepsilon = 24/p$ (for elastic electron-atomic collisions), $\lambda_\varepsilon = 2.6/p$ (for inelastic electron-atomic collisions), $R_{\mathrm{Le}} = 3.4\times 10^{-6}\sqrt{\varepsilon}/B$, and $R_{\mathrm{Li}} = 6.5\times 10^{-4}\sqrt{\varepsilon}/B$. Here, gas pressure p is in Pa, lengths in m, ε in eV, and B in T. Then, in the absence of a magnetic field, for a probe with $R = 0.1$ mm, and $p < 30$ Pa, ions are in the collisionless regime and for $p > 100$ Pa they are in the hydrodynamic regime. Electrons are in the collisionless regime if $p < 800$ Pa. If $p > 40\,000$ Pa, electrons are in the hydrodynamic regime. In the intermediate pressure range ($3000 < p < 15\,000$ Pa) electrons are in the nonlocal regime. Thus, for electrons the hydrodynamic regime is valid for pressures of order of atmospheric while for ions it is valid for pressures three orders less than atmospheric. In neon the electrons have

$\lambda_{ch} > \lambda_\varepsilon$, and ionization and recombination are not important for probe current collection in the collisionless and nonlocal regimes.

For magnetized plasma and magnetic field weaker than $B < 0.004$ T electrons with energy 16 eV will be in the collisionless regime I (for a probe perpendicular to the magnetic field). For $0.04 < B < 0.4$ T they will be in the nonlocal regime II.

5. Local and nonlocal concepts

The kinetic description of plasma depends on the ratio between the plasma inhomogeneity scale $\mathcal{L}$ and energy relaxation length λ_ε. The nonlocal approach is particularly important for the study of the EDF which is a solution to the Boltzmann kinetic equation.[26,42]

For the details of the nonlocal approach the reader is referred to the reviews.[34,45] Below we briefly describe the main idea.

If $\mathcal{L} \gg \lambda_\varepsilon$, a local approach is appropriate. The local approach assumes that spatial derivative can be ignored when solving the Boltzmann equation. The energy gain from the electric field is, therefore, *locally* balanced by energy loss in elastic and inelastic collisions with neutral particles. In this case, the EDF is determined by the local parameters. The argument of the local EDF is the speed v or kinetic energy ε. The distribution of $n_e(r)$ and the radial electric field are determined by the solution of the ambipolar diffusion equation.[26,45]

The nonlocal approximation is applicable in the opposite case $\mathcal{L} \ll \lambda_\varepsilon$, i.e., if electron diffusion in configuration space is much faster than the energy change due to collisions. The nonlocal kinetics implies that spatial derivatives must be retained in the Boltzmann equation.

As discussed above, in elastic collisions an electron changes direction of motion but does not significantly change kinetic energy. Inelastic collisions are rare compared to elastic ones since the inequality $\nu^* \ll \nu_a$ holds for most gases. Since the spatial displacement of electrons in this case is much faster than the energy gain and losses, the whole volume (the volume defined by the inhomogeneity scale $\mathcal{L}$) available for electrons contributes to the EDF formation.

Given that the total energy (kinetic plus potential) is approximately conserved during the motion, it is useful to include the quasistationary field in the total energy $W = \varepsilon - e\phi$ and to consider the EDF as a function of $(W, \mathbf{r})$ rather than of $(v, \mathbf{r})$. Here, ϕ is the plasma potential. For the same reason, the energy distribution at a certain point of space is determined by not only plasma parameters at this point but also by parameters of the remaining plasma, i.e., the energy distribution function at given point contains information about the energy distribution at any point within distance λ_ε (information about the directed part of distribution is lost due to collisions). In the nonlocal case the EDF cannot be represented as product of a function of the coordinates and a function of the velocity.

Neglecting possible nonlocality of the distribution causes not only quantitative but also qualitative errors, since application of the local approach for the $\mathcal{L} \ll \lambda_\varepsilon$ case leads to loss of information about how the distribution depends on spatial coordinates.

By applying these ideas to probes in plasmas we note that the inhomogeneity scale length $\mathcal{L} \approx d + h$ is that introduced by the probe. Nonlocality corresponds to $d + h \ll \lambda_\varepsilon$.

B. Basic models for the probe operation regimes

First, we will discuss briefly the main models for each regime in the absence of a magnetic field. For the collisionless regime the charged particle motion through the presheath is ballistic. Case I(a) of Table I (orbital motion limit) has been investigated by Mott-Smith and Langmuir.[3] For instance, for a cylindrical probe, it has been shown that for Maxwellian distributions and attracted particles the probe current density is

$$|j_{e,i}| = \frac{e n_e \bar{v}_{e,i}}{4} \frac{2}{\sqrt{\pi}} \left(\sqrt{\frac{e|V|}{T_{e,i}}} + \frac{\sqrt{\pi}}{2} \exp\left(- \frac{e|V|}{T_{e,i}} \right) \times \left[1 - \mathrm{erf}\left(\sqrt{\frac{e|V|}{T_{e,i}}} \right) \right] \right). \quad (11)$$

Here, V is the probe potential and $\bar{v}_{e,i} = \sqrt{8 T_{e,i} / \pi m_{e,i}}$. This expression gives the upper limit for the probe current in the collisionless regime, as potential barriers arising in the probe disturbed region can only reduce currents. The domain of validity of the orbital motion limit regime for cylindrical probes has been investigated in Refs. 46 and 47.

The cases of attracted electrons and ions in the regime I(b) and transition conditions between I(a) and I(b) have been considered in.[5–10,48–55] Laframboise[55] carried out extensive numerical computations of ion and electron collections for the collisionless regime. Several approximate fits to his results have been made.[10,56–59] For $e|V|/T_e \gg 1$ and $T_i/T_e \ll 1$ the collected ion current has a simple form

$$I_i = c e n_i \sqrt{\frac{2T_e}{m_i}} S_p, \quad (12)$$

where S_p is a probe area.[4,5] For the case of thin sheath $c = 0.4$ [regime I(b)]. For thicker sheaths [transition from regime I(b) to I(a)] c increases towards a number in excess of 1.0.[60]

A cross check of the models discussed above and comparison with results from alternative diagnostics (microwave, Druyvesteyn methods) have lead to estimates of the limits of their validity (see, for example, Refs. 60–63). A parametrization and iteration scheme permitting rapid analysis of probe data was provided in Ref. 60.

The case of repulsed particles in the collisionless regime will be considered in detail in Sec. III A. In the regime I(b) charged particles reach the probe surface conserving their energies and momentum. Therefore, in that case, it is possible to measure velocity and energy distributions in isotropic and anisotropic plasmas. In case I(a) it is possible to measure energy distributions only in isotropic plasma. In anisotropic plasma a spherical probe for the case of the spherical-symmetric sheath can also provide such measurements. In regime I distribution functions are proportional to

the second derivatives of electron or ion probe currents with respect to the probe voltage $d^2I_{e,i}/dV^2$ [Druyvesteyn Eq. (27)[64]].

To our knowledge, the nonlocal regime for attracted electrons has not yet been investigated. In isotropic plasmas, case II(d) for repelled electrons was investigated in Ref. 43. In this approach the Boltzmann kinetic equation (reduced to a diffusion equation) was solved (see Sec. III A for details). The solution yields the electron energy distribution, being proportional to the first derivative of the electron current dI_e/dV. This is also valid for subregimes (b) and (c) of the case II since the model depends weakly on the sheath thickness.[21] However, for subregime II(a) the Druyvesteyn Eq. (27) should be used.

In experiments it is always possible to change the probe radius and thus to choose between regimes I and II. Nevertheless, it is useful to develop a theory, which covers both regimes, the so-called kinetic theory. Such a model allows a study of the transition between diffusive and collisionless particle motion and gives more exact conditions for their validity.[21,36,65,66] The first attempt to take into account collisions for regime I was made by Swift.[67] Later a more general theory of electron sink to the probe has been developed in Ref. 68. The theory gives results which are very similar to the more exact model based on a solution of the kinetic equation.[21,69,70]

In the hydrodynamic regime particle collection is described by transport equations for which the information about the energy distributions is lost completely. This gives an upper limit on gas pressure for which the EDF and IDF measurements can be performed. In this regime it is only possible to measure fluid observables (see, for example, Refs. 10, 14, 16, 19, and 24). Note that λ_i is usually much less than λ_e, hence electrons may be in the collisionless or nonlocal regime while ions are hydrodynamic. An example of such a case (for the EDF of an arbitrary form) was studied in Refs. 10, 37, and 71, where the following formula connecting certain plasma parameters and the ion current to a cylindrical probe was derived:

$$n_e(T_i+7700\langle\varepsilon\rangle)=1.3\times10^{17}\frac{R}{\lambda_i}\sqrt{m_iT_i}j_i\ln\left(\frac{\pi L}{4\rho_i}\right). \quad (13)$$

Here $\langle\varepsilon\rangle$ is the mean kinetic energy (in eV) of the electrons in the undisturbed plasma with the density n_e, T_i is ion temperature given in Kelvin, n_e in m^{-3}, m_i in amu, and j_i in A/m^2. The radius of the sheath ρ_i can be found, for instance, from formulas given in Sec. II A.

A detailed description of hydrodynamic models can be found in Ref. 24.

In the magnetized plasma, despite numerous theoretical and experimental studies, the theory of the probes is still far from complete.[72–74] Below we review the main theories developed for those regimes that fall within the scope of this article (see discussion in Sec. I).

In the case of $\lambda_{e,i}\ll R_{\mathrm{Le},i}$ the magnetic field has weak influence on the charged particle motion. For $R_{\mathrm{Le}}\gg R$, h and regime I(a) the effect of magnetic field for attracted electrons is negligible and the orbital motion limit theory can be applied.[46] For repelled particles in regime I it has been shown[5] that unmagnetized theory is valid for $R_{\mathrm{Le},i}\gg L$ if the probe is oriented parallel to the magnetic field, and for $R_{\mathrm{Le},i}\gg R\ln(L/R)$ if the probe is oriented perpendicular to the field.

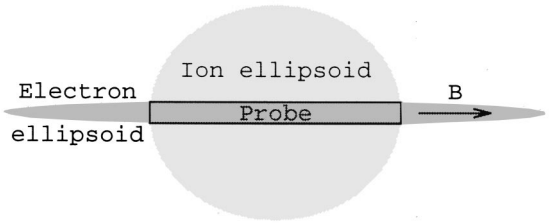

FIG. 4. Regions from which electrons (electron ellipsoid) and ions (ion ellipsoid) are drawn to the probe. B is the direction of the magnetic field.

The condition for nonlocal regime in magnetized plasma is $\lambda_{\varepsilon\perp}\gg d_\perp+h\gg R_{\mathrm{Le}}$. The regime for repelled electrons has been investigated in Ref. 43. The transition between collisionless and nonlocal regimes has been examined in Refs. 21, 68, and 70 (see, Sec. III A).

Hydrodynamic models for electron current in magnetized plasma give similar results for both weakly ionized[4,44,75–77] and fully ionized[16,44,73,78] plasmas if the probe is small.[44] By small we mean probes with size perpendicular to the magnetic field comparable to the ion gyro radius. These models describe the electron collection as a diffusion process with classical[16,44,73,75] or anomalous[16,78] diffusion coefficients. In Ref. 79 the model for current was based on rigorous and complicated kinetic description which led to the discovery of so-called potential overshoot, a nonmonotonic potential profile near the probe. This effect was introduced heuristically (with reference to Ref. 79) in the hydrodynamic models mentioned above. Models for the ions in the hydrodynamic regime in weakly ionized magnetized plasma are similar to those for electrons, i.e., are governed by diffusion.[44,75–77]

There are situations in magnetized plasma where transport processes due to other mechanisms than classical (collisional) particle diffusion should be taken into account. Some authors include the energy equation in the hydrodynamic models, giving importance to temperature gradients near the probe.[74] Other transport processes considered are transverse conductivity due to ion inertia, ion viscosity,[72,80,81] and anomalous diffusion and viscosity.[16,78,82,83] As mentioned in Sec. I, probe methods based on hydrodynamic theories that require the inclusion of these more subtle transport processes, will not be reviewed systematically in this article.

As an illustration, let us consider the diffusion model for weakly ionized magnetized plasma.[75] The model is valid for a parallel oriented cylindrical probe satisfying the conditions $R_{\mathrm{Le},i}\ll R$ and

$$\frac{L}{2x_e}<R<\frac{L}{2(1+x_i^2)^{1/2}}. \quad (14)$$

In this regime, the plasma density is disturbed by the probe in an ellipsoid with semi-axes (R,Rx_e) (electron ellipsoid) in electron saturation and in an ellipsoid with semi-axes $[L/(2(1+x_i^2)^{1/2}),L/2]$ (ion ellipsoid) in ion saturation. A sketch of these ellipsoids are shown in Fig. 4. Both ion and

electron saturation currents are governed by classical diffusion, and according to Ref. 77 the ion saturation current is

$$I_i^{\rm sat}=\frac{8\pi en_e(1+T_e/T_i)D_i(\gamma_i^2-1)^{1/2}}{\ln[1+(1-\gamma_i^{-2})^{1/2}/1-(1-\gamma_i^{-2})^{1/2}]}\ \frac{R}{(1+x_i^2)}. \tag{15}$$

Here D_i is ion diffusion coefficient (along the magnetic field), n_e is the unperturbed plasma density, and $\gamma_i = L/[2R(1+x_i^2)^{1/2}]$. The electron current is the Bohm saturation current[77]

$$I_e^{\rm sat}=-\frac{4\pi en_e(1+T_i/T_e)D_{e\perp}x_eR(1-\gamma_e^2)^{1/2}}{\arctan(1-\gamma_e^{-2})^{1/2}}. \tag{16}$$

Here, $D_{e\perp}$ is the electron diffusion coefficient perpendicular to the magnetic field and $\gamma_e=L/(2Rx_e)$. In the limit $L \ll Rx_e$ and $T_i \ll T_e$ this equation takes the simple form

$$I_e^{\rm sat}=-\frac{8n_eRT_e}{B}, \tag{17}$$

where B is the magnetic field.[84] The construction of the transition part of the characteristic is similar to other diffusive models.[16,73] This is done by relating the potential overshoot[79] in the sheath to the particle fluxes to the probe from the plasma. Defining β as the the ion current normalized by the ion saturation current, $I_i=\beta I_i^{\rm sat}$, we can find β (for a thin sheath) as a function of probe voltage V from the expression

$$\mathrm{eV}=T_i\ln\left[\frac{2\pi en_eRL\overline{R}_{\rm Li}\overline{\nu}_i(1-\beta)}{\beta I_i^{\rm sat}}\right]+T_e\ln(1-\beta), \tag{18}$$

where $\overline{R}_{\rm Li}$ is the average ion Larmor radius and $\overline{\nu}_i$ is the average ion collision rate, $\overline{R}_{\rm Li}\overline{\nu}_i \approx \sqrt{T_i/(2m_i)}$ for $x_i<1$ and $\overline{R}_{\rm Li}\overline{\nu}_i \approx \sqrt{T_i/(2m_i)}/x_i$ for $x_i>1$.[85] Similarly α, defined by $I_e=\alpha I_e^{\rm sat}$, can be found from the equation

$$\mathrm{eV}=-T_e\ln\left[\frac{\pi en_eR^2\overline{v}_e(\alpha-1)}{\alpha I_e^{\rm sat}}\right]-T_i\ln(1-\alpha). \tag{19}$$

Equations (18) and (19) are solutions for the case of a thin sheath, similar equations for the case of thick (diffusion) sheath can be found in Ref. 75.

If $2R>L(1+x_i^2)^{-1/2}$, the ion density is perturbed inside the electron ellipsoid. The expression for the ion saturation current will coincide with that for electrons [Eq. (16)], where the subscript e is replaced by i, and Eq. (18) is no longer valid. Since the ion saturation current is very small compared to the electron saturation current, it is possible to describe almost the entire characteristic by Eq. (19).[44]

C. Sources of errors

A large number of nonideal effects may create errors in probe measurements.[6,9,17,21] Each of them has to be examined carefully for particular plasma conditions and a given experimental setup. Application of theories, which are invalid for the regime given by the plasma conditions and the probe construction, is a common source of error. For instance, employment of models for unmagnetized plasma in the presence of magnetic fields may yield significant errors (one order of magnitude) in the density measurements.[35] Below we discuss a few common errors and how they can be remedied. More detailed discussion of errors associated with particular probe techniques will be given in those sections where the techniques are described.

1. Influence of probe holder

All probes are mechanically attached to an insulating probe holder, with the exception of the case when the probe is a part of the vessel wall. The area of the holder surface may be much larger than the area of the probe, hence it can influence the plasma much more than the probe tip itself. Therefore, the holder design should be chosen to minimize the perturbation of the local plasma properties and probe measurements. Figures showing examples of bad and good probe designs can be found in Ref. 17. Holder dimensions smaller than $\lambda_{e,i}$ provide the least plasma distortion.

In a magnetized plasma the orientation of the holder plays an important role. To avoid shadowing effects it is advisable to orient the probe holder perpendicular to the magnetic field lines. To orient both probe tip and probe holder parallel to the field is not recommended.

In general, for estimating the influence of the holder a kinetic equation for plasma with a new boundary must be solved. Unfortunately, it can be done only for special cases. For example, in Ref. 86 an estimate of the distortion of electron density by holders in unmagnetized plasma is provided. In this work simple holder geometry and a diffusive regime for electrons were assumed.

2. Influence of a dirty probe surface

Impurities on the probe surface may contaminate the plasma. They can also provide favorable conditions for reflection and secondary emission of electrons from the probe surface, leading to distortion of the $I-V$ characteristic.[87] Note that the effects of secondary emission can be important even for clean probe surface in plasmas with $T_e>15$ eV.[88,89] These effects become particularly important for measurements under complex plasma conditions. The growth of films on the probe surface in chemically active plasma can be an illustration.

The measurement of charged particle distributions is very sensitive to such effects.[90,91] Figure 5 presents the energetic part (9–13 eV) of the EDF measured by a molybdenum probe in a neon afterglow plasma.[91] Curve 1 shows the EDF measured by a probe which was cleaned by the ion saturation current before the measurements. The maximum on the curve is due to the fast electrons born in pair collisions of metastable neon atoms. Curve 2 demonstrates the same measurements conducted with a dirty probe. In this case a spurious negative EDF was observed. Note that cleaning of the metallic probe by the electron saturation current might lead to significant errors in EDF measurements due to hardening of the probe surface. Constructions of direct and indirect heated probes can be found, for example, in Refs. 92–94.

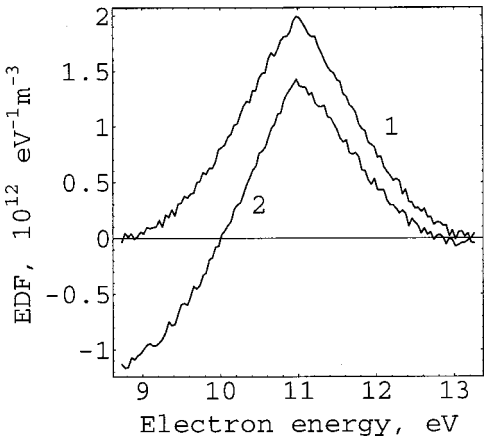

FIG. 5. Measured EDF in neon afterglow plasma with a molybdenum probe, $R=0.044$ mm. Gas pressure was 130 Pa. "Clean" probe (1) and "dirty" probe (2).

3. Uneven work function over the probe surface

The work function of the probe material can vary at different locations of its surface, for instance due to the polycrystalline structure of the probe.[9,95] This might create an uncertainty in determination of the probe potential. Usually the difference does not exceed a few hundredth of eV. The presence of such an effect will cause a broadening of the measured probe characteristic of the order ~0.1 eV. This becomes an important effect when measuring very low electron or ion temperatures ($T_{e,i}<0.1$ eV), for example, in afterglow plasmas.

4. Finite resistance between reference electrode and plasma

When we bias the probe we assume that the plasma potential stays constant, i.e., it is not dependent on the magnitude of the probe current. However, the plasma between the probe and the reference electrode can have a finite resistance R_p, and the voltage drop V_R through the sheath of the reference electrode can depend on the probe current I, say $V_R = V_{R0}+R_R I$. For this circuit the plasma potential in front of the probe (relative to the potential of the reference probe) is $V_p=V_{R0}+(R_p+R_R)I$. Care should be taken to reduce the current dependent voltage drop $(R_p+R_R)I$ to a level where it can be neglected. Normally this can be done by miniaturizing the probe tip (reducing I) and employing a large reference electrode (reducing R_R). In cases where this does not work, for instance if the probe for some reason is large, a small tracking electrode in vicinity of the probe can be used to monitor the dependence of the plasma potential with I.[21,96]

5. Oscillations of the plasma potential

Distortion of the probe characteristic (and its derivatives, see Sec. III) due to plasma potential oscillations ($\tilde{V}_p$) can occur in noisy or rf exited plasmas. This is caused by the nonlinear shape of the characteristic in the transition region. Such distortions of the characteristic have been studied since the 1960s.[97–101] In noisy plasmas it is necessary to average the characteristic over many sweeps in order to obtain a smooth curve. For $e\tilde{V}_p \geqslant T_e$ the averaging will lead to a broadening of the transition region and to an overestimate of temperature if this region is used for this estimate. For large negative potentials with respect to the plasma potential (around the floating potential) the characteristic is not disturbed significantly and can more reliably be used to determine T_e. The effect of plasma potential fluctuations can be studied by introducing the fluctuating part of the potential (for example, as a sine or square wave) into an analytical model for the $I-V$ characteristic. Visual examples of such modeling can be found in Refs. 15 and 102. To avoid distortion of the characteristic in noisy or rf plasmas the interfering ac voltage in the probe sheath must be eliminated by a compensation circuit. Different methods, depending on the frequency spectrum of the interfering voltage, are reviewed in Refs. 15 and 17 (see, also Refs. 103–107).

6. Influence of I_e on the measurements of I_i and vice versa

Plasma parameters can be extracted from either I_e or I_i. Only the saturation parts of the characteristic (at large negative or positive V_p) are completely dominated by either I_i or I_e. In the transition part of the characteristic the probe current is the sum of the ion and electron components $I=I_e+I_i$. Thus, if the transition part is employed for measurements of T_e, T_i and charged particle velocity distributions, I_e and I_i, should be separated. The linear or power extrapolation of the ion current is the simplest approach and often used in practice. In general, a particular model of ion current for actual conditions may be applied for such an extrapolation.

A theoretical investigation of the influence of the ion probe current on the EDF measurements was carried out in Refs. 108 and 109. In these works a collisionless theory[39] was applied. It has been shown, for example, that for a Maxwellian EDF the ion current does not perturb probe measurements for $\varepsilon<6T_e$.

An analogous calculation can be made for higher pressure plasma when $\lambda_i<d+h$. In this case the ion probe current can be calculated by applying formulas from Refs. 10 and 71. Such computations allow us to estimate the energy range where the measurements of the EDF are reliable.

The influence of the ion current increases with magnetic field. This is due to the fact that the current ratio I_e/I_i decreases. That may lead, for instance, to the emergence of additional false maxima of the measured EDF.[110]

Measurements by probes of different radii may be very useful with respect to improving accuracy.[111] For the case $\lambda_i<d+h$ it allows us to improve the measured EDF. In this case I_i'' is independent of the probe radius. At the same time I_e'' is proportional to the probe radius. Therefore, the subtraction of the I'' measured by probes of different radii yields us the real I_e''.[71] Figure 6 represents the measurements of the EDF in Ne afterglow plasmas by probes of different radii.

7. The instrumental functions in probe measurements

The influence of some instrumental spurious effects on the probe measurements of I, I', and I'' can be estimated by applying so-called instrumental functions.[12,23,90,112–114] The

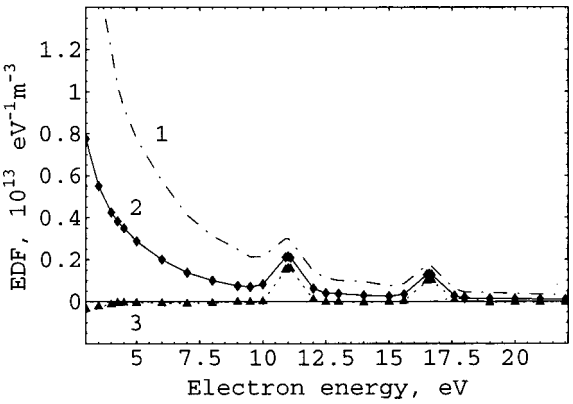

FIG. 6. EDF in neon afterglow plasma. Curves (1) and (2) are the EDF calculated with Eq. (27) from measured I''. Curve (3) is the corrected EDF. Curves (1) and (2) are from the probes with $R=17.5$ and 44 μm, respectively. After Ref. 71.

results of a measurement I_m (similar for I'_m and I''_m) is given as the convolution of the true I and an instrumental function $\mathcal{A}$:

$$I_m(V)=\int_{-\infty}^{\infty} I(V_1)\mathcal{A}(V_1-V)dV_1\equiv I*\mathcal{A}. \tag{20}$$

The true functions I, I' and I'' may be extracted from I_m, I'_m and I''_m by solving Eq. (20).[114,115] In the presence of l different spurious effects, each described by an instrumental function $\mathcal{A}_k$, $k=1,...,l$, the function $\mathcal{A}=\mathcal{A}_1*\mathcal{A}_2*\ldots*\mathcal{A}_l$ provides the description of the total distortion of the measurement. A large number of instrumental functions have been described in the literature.[12,23,90,113,116,117] Some arise from the finite time of measurements,[12,118] others from reflection and secondary emission of electrons from the probe surface,[90,91] and a third category is due to oscillations of plasma potential.[102] Based on results of these works, the comparison between different methods of measurements of the EDF was made in Ref. 116.

The instrumental functions can be measured[21,91] and allow estimates of the overall accuracy of a given probe measurement. The state of the art in EDF measurements is a few percent accuracy in the relative EDF and 10%–15% in the absolute values.

III. MEASUREMENT OF CHARGED PARTICLE DISTRIBUTIONS

This section reviews methods for measurement of charged particle velocity distributions. The state of the art of this field is that it is possible to determine isotropic and anisotropic electron velocity distribution functions in low-pressure plasmas (up to some hundreds of Pa) and also to measure electron energy distribution functions at high pressure (up to tens of thousands of Pa) and in magnetized plasmas. Information about the energy distribution of ions can also be obtained in some cases. The results presented in this section are valid only for repulsive probe potential for the particle species under consideration.

A. Measurements of EDF

A number of methods exist for measurement of the electron energy distribution function. It is possible to recover the EDF from optical emission spectra.[24,119–121] In Ref. 122 an optical probe has been proposed for such measurements. A directional velocity analyzer has been suggested in Ref. 123 for the measurements of the anisotropic function. However, the single electric probe is a widely used instrument for EDF measurements.

1. Measurements of isotropic EDF

In unmagnetized plasma the connection between the EDF and probe current is simple in two limits; the collisionless regime[5–9,11,12,17,21,24,25] and the nonlocal regime.[21,43] In a transition regime approximate solutions[21,68,70] exist and allow us to estimate errors of both limits. Measurements by a nonspherical probe with different orientations permit confirmation of the isotropy (or weak anisotropy) of the EDF.

In a weakly magnetized plasma and $R_{\mathrm{Le}}\gg L$ (for the parallel cylindrical probe) or $R_{\mathrm{Le}}\gg R\ln(L/R)$ (for the perpendicular probe) the formulas for the collisionless regime are valid if $\lambda_e\gg d$.

In a strongly magnetized plasma ($\lambda_{\varepsilon\perp}\gg R\gg R_{\mathrm{Le}}$) the same approaches as for the nonlocal regime[35,43] can be applied. In a magnetized plasma, approximate solutions for the transition regime ($d_\perp\sim R_{\mathrm{Le}}$) have also been developed,[21,68,70] but not yet verified experimentally.

As the purpose of the probe measurement is to recover the unperturbed distribution function, the connection between the distribution function on the probe surface and in the undisturbed plasma must be found. This connection is provided by solutions of the Boltzmann equation[26]

$$\frac{\partial f}{\partial t}+\mathbf{v}\cdot\nabla f+\frac{e}{m_e}(\mathbf{E}+\mathbf{v}\times\mathbf{B})\cdot\nabla_v f=S \tag{21}$$

in the region disturbed by the probe. Here ∇ is the gradient in configuration space, ∇_v in velocity space, $\mathbf{E}$ and $\mathbf{B}$ are electric and magnetic fields, and S is a collision term. The method of solving this equation depends on the probe operation regime.

a. Collisionless regime [$\lambda_e\gg d+h$ *for unmagnetized plasma, and* $R_{\mathrm{Le}}\gg L$ (*parallel probe*) *or* $R_{\mathrm{Le}}\gg R\ln L/R$ *perpendicular probe*) *for magnetized plasma*]. In this case there are no collisions in the region disturbed by the probe, i.e., $S=0$ and Eq. (21) reduces to the Vlasov equation $df/dt=0$.[26] This states that the distribution function (phase-space density) is conserved along its phase-space trajectory. Consider a phase-space point $(\mathbf{r}_s,\mathbf{v}_s)$, where $\mathbf{r}_s$ is a point on the probe surface and $\mathbf{v}_s$ is a velocity whose component along the directional normal points into this surface. If the probe surface is convex, and the potential is repulsive, the corresponding phase-space trajectory can, in principle, be traced backwards in time until it ends up in the undisturbed plasma. Let us represent an arbitrary point on this trajectory in the undisturbed plasma by $(\mathbf{r},\mathbf{v})$. The conservation of phase-space density implies that

$$f(\mathbf{r}_s,\mathbf{v}_s)=f(\mathbf{r},\mathbf{v}), \tag{22}$$

where $f(\mathbf{r},\mathbf{v})d^3rd^3v$ denotes the number of particles in the phase-space volume d^3rd^3v. If the velocity distribution in the undisturbed plasma is isotropic and spatially homogeneous, the phase-space density depends only on $v\equiv|\mathbf{v}|$, or equivalently, on the kinetic energy $\varepsilon=mv^2/2$. As discussed in Sec. II A, for $d\ll\lambda_\varepsilon$ the total energy $W=\varepsilon-e\phi(r)$, is approximately conserved along the trajectory through the disturbed region. Thus $W=\varepsilon=\varepsilon_s-eV$. Then the right-hand side of Eq. (22) can be written $f(\varepsilon_s-eV)$, and by representing $\mathbf{v}_s$ in terms of the kinetic energy ε_s and two angles θ_s and φ_s, Eq. (22) can be written in the form

$$f(\mathbf{r}_s,\varepsilon_s,\theta_s,\varphi_s)=f(\varepsilon_s-eV). \tag{23}$$

Here, θ_s is the angle between $\mathbf{v}_s$ and the directional normal $\hat{\mathbf{n}}_s$ pointing into the probe surface, and φ is the azimuthal angle around the axis along $\hat{\mathbf{n}}_s$.

For a convex probe surface the electron current density can be expressed as

$$j_e=|\mathbf{j}_e|=-e\int \mathbf{v}_s\cdot\hat{\mathbf{n}}_s f(\mathbf{r}_s,\mathbf{v}_s)d^3v_s, \tag{24}$$

where the integration is performed over the half-space for which $\mathbf{v}_s\cdot\hat{\mathbf{n}}_s>0$. Performing the integration in the polar coordinates (v_s,θ_s,φ_s), using Eq. (23), and changing to the integration variable $W=\frac{1}{2}mv_s^2-eV$, yields

$$j_e=-\frac{2\pi e}{m^2}\int_{-eV}^{\infty}(W+eV)f(W)dW, \tag{25}$$

known as the Langmuir formula. In the case of Maxwellian distribution function this equation takes the simple form

$$j_e=en_e\sqrt{T_e/(2\pi m_e)}\exp(-eV/T_e). \tag{26}$$

Differentiating Eq. (25) twice we obtain the Druyvesteyn formula[64]

$$f(\varepsilon=-eV)=-\frac{m_e^2}{2\pi e^3}\frac{d^2j_e}{dV^2}. \tag{27}$$

Thus, in this case the EDF is proportional to the second derivative of j_e with respect to the probe potential. Equation (27) has been verified and applied in numerous experiments.[2–6,8,9,11,16]

For example, Fig. 7 presents the result of measurements of the EDF in energy space $f_\varepsilon(\varepsilon)$ obtained by the Druyvesteyn method. The experiment was performed in a low-pressure (27 Pa) helium afterglow plasma[115] by a cylindrical probe with a radius $R=0.044$ mm and length $L=3$ cm (curve 1). The plasma was created by current pulses applied to cold electrodes in a glass tube with inner diameter 36 mm and length 22 cm. The pulses were of duration 10 μs, magnitude 0.2 A, and repetition frequency 2 kHz. The axis of the probe coincided with the axis of the discharge tube. The plasma decay time in the afterglow was $t_a=50\,\mu$s. The measured EDF was corrected by solving Eq. (20) (curve 2). The time resolution of the method was about 10 μs. The peaks on the EDF are due to ionization collisions of two metastable He* atoms with the creation of fast electrons.[124]

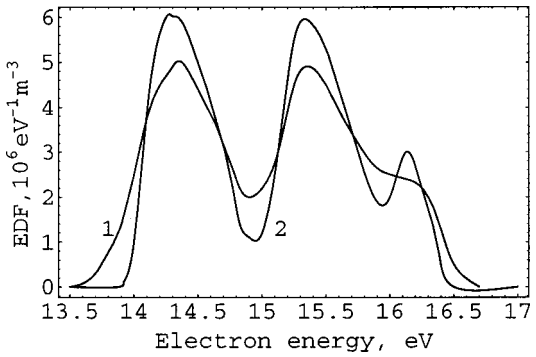

FIG. 7. EDF in energy (fast part) in a helium low-pressure (27 Pa) afterglow plasma. Magnitude of current pulses is 0.2 A, repetition frequency is 2 kHz, $t_a=50\,\mu$s, $R=0.044$ mm and $L=3$ cm. Curve (1) is EDF obtained by Druyvesteyn method. Curve (2) is the same corrected by solving Eq. (20). After Ref. 115.

This example illustrates the possibilities inherent in the method. Probes allow us to conduct investigations of elementary processes[125,126] (see Sec. V A).

b. Nonlocal regime, unmagnetized plasma ($\lambda_\varepsilon\gg d+h\gg\lambda_e$). In this case the electrons from the undisturbed plasma move to the probe in the diffusion regime conserving their total energy W but not the momentum. Since electrons undergo many collisions before they reach the probe, the EDF near the probe is weakly anisotropic, and hence the two term expansion (stationary case)

$$f(\mathbf{v},\mathbf{r})=f_0(v,\mathbf{r})+\frac{\mathbf{v}}{v}\cdot\mathbf{f}_1(v,\mathbf{r})=f_0(v,\mathbf{r})+f_1(v,\mathbf{r})\cos\vartheta \tag{28}$$

is valid.[26,42] Here $\mathbf{r},\mathbf{v}$ are coordinates in six-dimensional phase space for the electrons, $v=|\mathbf{v}|$, ϑ is the angle between $\mathbf{v}$ and $\mathbf{f}_1$, and $f_1(v)=|\mathbf{f}_1|$. It is important to note that the direction of $\mathbf{f}_1$, and hence the angle ϑ, depends on the speed v.

It is easy to show[26] that the expansion coefficients f_0 and $\mathbf{f}_1$ are the isotropic and directional parts of the EDF, and integrated over the velocity space these coefficients yield density and fluid velocity (and thus current), respectively. Let us normalize the EDF by the electron density n_e:

$$\int f(\mathbf{v},\mathbf{r},t)d\mathbf{v}=n_e(\mathbf{r},t), \tag{29}$$

and choose a spherical coordinate system with axis perpendicular to the probe surface and polar and azimuthal angles denoted as ϑ and φ, respectively. Here, the direction of the axis coincides with the direction of $\mathbf{f}_1$.

Substitution of the expansion (28) into the stationary Boltzmann equation, subsequent multiplication of the resulting equation by $d(\cos\vartheta)$ and $\cos\vartheta d(\cos\vartheta)$, and integration over angles, yield equations for f_0 and $\mathbf{f}_1$:

$$\frac{v}{3}\nabla\cdot\mathbf{f}_1-\frac{e}{3m_ev^2}\frac{\partial}{\partial v}(v^2\mathbf{E}\cdot\mathbf{f}_1)=S_0, \tag{30}$$

$$v\nabla f_0-\frac{e\mathbf{E}\partial f_0}{m_e\partial v}-\frac{e}{m_e}[\mathbf{B}\times\mathbf{f}_1]=\mathbf{S}_1. \tag{31}$$

To find the probe current we need to solve Eqs. (30) and (31) for $\mathbf{f}_1$ on the probe surface. Simple Krook collision terms, $S_0=\delta\nu_a f_0$ and $\mathbf{S}_1=-\nu_a\mathbf{f}_1$,[42,43] are used and the background electric field is neglected, so $\mathbf{E}=-\nabla\phi(\mathbf{r})$, where ϕ is the potential variation introduced by the probe. Note, in Eqs. (30) and (31) f_0 and $\mathbf{f}_1$ are functions of particle speed v and $\mathbf{r}$. Alternatively, we can change variables from v to ε in these equations and express the functions as $\hat{f}_0(\varepsilon,\mathbf{r})$ and $\hat{\mathbf{f}}_1(\varepsilon,\mathbf{r})$. Since $\hat{\mathbf{f}}_1\to 0$ as $r\to\infty$, we have that $\hat{f}_0(\varepsilon,r\to\infty)=f(\varepsilon)$. As this regime is nonlocal (energy is conserved in collisions), it is further useful to change variables from ε to $W=\varepsilon-e\phi$, so that we have $f_0(W,\mathbf{r})\equiv\hat{f}_0(\varepsilon,\mathbf{r})=\hat{f}_0(W+e\phi(\mathbf{r}),\ \mathbf{r})$. With this transformation of variables $\mathbf{f}_1$ can be eliminated from Eqs. (30) and (31), which in the region near the probe reduces to the stationary diffusion equation[43]

$$\left(\frac{\partial}{\partial\mathbf{r}}\right)_W\cdot\left[D_e(\mathbf{r})\cdot\left(\frac{\partial f_0}{\partial\mathbf{r}}\right)_W\right]=0, \tag{32}$$

where partial differentiation is with respect to $\mathbf{r}$ under constant W (not constant v). Here the diffusion coefficient $D_e=v^3/(3\nu_a)=(2\varepsilon/m)^{3/2}/(3\nu_a)$ is a function of the kinetic energy, but since $\varepsilon=W+e\varphi(\mathbf{r})$ is a function of space for constant W, we write that $D_e=D_e(\mathbf{r})$ in Eq. (32).

The boundary condition on a fully absorbing probe surface is $f_0(W,\mathbf{r}_s)=0$. This is an acceptable diffusive approximation[6,10,36,66] because the electron density at the surface is very small compared with its value in the undisturbed plasma where $f_0(W,r\to\infty)=\hat{f}_0(\varepsilon,r\to\infty)=f(\varepsilon)$.

For a spherical or cylindrical probes Eq. (32) becomes one-dimensional[10] and f_0 is a function of r, where r is a distance from the point in the plasma to the center of the spherical probe or to the axis of the cylindrical probe. The solution of Eq. (32) provides the probe current density

$$j_e=-\frac{8\pi e}{3m_e^2}\int_{-eV}^{\infty}\frac{Wf_0(W)dW}{\Psi(W,V)}, \tag{33}$$

where $f_0(W)\equiv f_0(W,r\to\infty)$ and the diffusion parameter Ψ is

$$\Psi(W,V)=\frac{1}{\lambda_e}\int_R^A\frac{\sqrt{W}D_e(W)dr}{(r/R)^{\Upsilon}\sqrt{W+e\phi(r)}D_e[W+e\phi(r)]} \tag{34}$$

and $\Upsilon=1$, $A=\pi L/4$ for the cylindrical probe and $\Upsilon=2$, $A=\infty$ for the spherical probe. From Eq. (34) we observe that, in general, it is necessary to know the profile of the near-probe potential $\phi(r)$, which can be calculated by solving jointly the equation of motion for ions and the Poisson equation.[10,75]

For a thin sheath ($h\ll d$) we have that $\phi(r)\approx 0$ throughout most of the integration volume, and can be neglected in Eq. (34). The same simplification of the integral for Ψ is obtained for $vD_e=\text{const}$ (argon plasma) for any h. In both cases Eq. (33) reduces to

$$j_e=-\frac{8\pi e}{3m_e^2R\kappa}\int_{-eV}^{\infty}\lambda_e(W)Wf_0(W)dW, \tag{35}$$

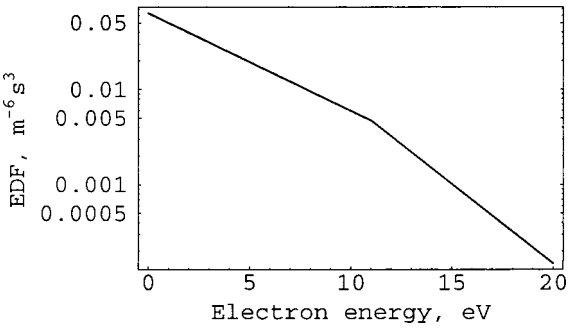

FIG. 8. EDF in velocity in a strongly magnetized (0.3 T) helium low-pressure (0.2 Pa) plasma. $R=0.25$ and $L=5$ mm. After Ref. 35.

where $\kappa=\ln(\pi L/4R)$ for the cylindrical probe and $\kappa=1$ for the spherical probe. The following equation has been obtained from Eq. (35):[43]

$$f(\varepsilon=-eV)=f_0(W=-eV)=\frac{3m_e^2R\kappa}{8\pi\lambda_e(-eV)Ve^3}\ \frac{dj_e}{dV}. \tag{36}$$

The influence of sheath thickness h on the measurements can be investigated by solving model problems. It was shown in Refs. 21 and 70 that in regimes II(b) and II(c), Eqs. (35) and (36) are still valid for a very thick sheath ($h\sim 30R$). In this case the errors are small for energies higher than T_e. For regime II(a) ($\lambda_\varepsilon\gg h\gg\lambda_e\gg d$) the Druyvesteyn Eq. (27) should be used.

Thus, in diffusive regimes II(b), II(c), and II(d) the EDF can be determined from the measured dI_e/dV independently of the sheath thickness and in II(a) from dI_e^2/dV^2. Equation (36) has been applied for EDF measurements in Refs. 43, 127, and 128.

c. Nonlocal regime, strongly magnetized plasma [$\lambda_\varepsilon(R_{\mathrm{Le}}/\lambda_e)\gg R\gg R_{\mathrm{Le}}$]. In this case Eq. (32) remains valid but the diffusion coefficient is replaced by a tensor.[26,42] This equation was solved in Ref. 43 for a cylindrical probe oriented along the magnetic field. The near-probe sheath was assumed to be thin. With boundary conditions similar to the previous (unmagnetized) case, the solution of Eq. (32) yields

$$I_e(V)=-\frac{64\sqrt{2}\pi eR}{3\omega_e m_e^{5/2}}\int_{-eV}^{\infty}W^{3/2}f_0(W)dW, \tag{37}$$

where ω_e is the electron cyclotron frequency. From this expression the EDF can be found as

$$f_0(W=-eV)=\frac{3\omega_e m_e^{5/2}}{64\sqrt{2}\pi e^2R(eV)^{3/2}}\ \frac{dI_e}{dV}. \tag{38}$$

A similar formula for a perpendicular oriented probe has been obtained in[35]

$$f_0(W=-eV)=\frac{3m_e^2\ln(\pi L/4R)}{16\pi^2e^3VR_{\mathrm{Le}}}\ \frac{dI_e}{dV}, \tag{39}$$

where R_{Le} is Lazmore radius of an electron with energy eV. In Ref. 21 it was demonstrated that Eqs. (38) and (39) are still valid for the case of thick sheath $h\gg R$. Thus, in the case of strongly magnetized plasma, the EDF is proportional to the first derivative of I_e. This resembles the situation in a high-pressure plasma. For example, Fig. 8 presents the result

of measurements (after Ref. 35) of the EDF in velocity space (as a function of ε) in a strongly magnetized ($\sim$0.3 T), low-pressure ($\sim$0.2 Pa) helium plasma. The cylindrical probe had radius $R=0.25$ mm and length $L=5$ mm. Equations (38) and (39) were applied to the measured I-V characteristics. From the figure it appears that the measured EDF is a two-temperature Maxwellian with suppressed tail. It seems that a theoretical model developed for these conditions can predict such a tail of EDF.[129]

d. The transition regime for unmagnetized plasma ($\lambda_e \sim d$). In this case the EDF near the probe deviates strongly from spherical symmetry and thus, expansion (28) is not valid. To calculate the probe current the solution of the full kinetic equation (21) is required, which is a very complicated problem. The situation is analogous to the Milne problem,[130] which has been investigated in the theory of radiation transfer in stellar atmospheres, neutron transfer in nuclear reactors,[36,66] and diffusion of charged particles in gases.[36,65,131,132] In those articles it was demonstrated that the approximate electron current can still be obtained from the diffusion equation (32), but with special boundary conditions on the probe surface:

$$f_0(W,R)=\gamma_0 f_1(W,R)=-\gamma_0\lambda_e\left(\frac{\partial f_0}{\partial r}\right)_W. \tag{40}$$

Here, γ_0 is a geometrical factor depending on R/λ_e. For isotropic scattering in unmagnetized plasma γ_0 decreases monotonically from 4/3 to 0.71 as R/λ_e increases from 0 to ∞. The detailed behavior of γ_0 between these limits was calculated in Ref. 66. For the cylindrical probe γ_0 can be approximated as follows:[35]

$$\gamma_0=\frac{4}{3}-0.62e^{-\lambda_e/2R}. \tag{41}$$

The solution of Eq. (32) with boundary conditions given by Eq. (40) yields

$$j_e=-\frac{8\pi e}{3m_e^2}\int_{-eV}^{\infty}\frac{(W+eV)f_0(W)dW}{\gamma_0+(1+eV/W)\Psi(W,V)}, \tag{42}$$

where the expression for $\Psi(W,V)$ is the same as Eq. (34). For the case $\upsilon D_e=\text{const}$ or $h\ll d$, Eq. (42) reduces to

$$j_e=-\frac{8\pi e}{3m_e^2}\int_{-eV}^{\infty}\frac{(W+eV)f_0(W)dW}{\gamma_0+(R\kappa/\lambda_e)(1+eV/W)}. \tag{43}$$

For $\lambda_e \gg d$, Eq. (43) reduces to Eq. (25) (collisionless regime) and for $\lambda_e \ll d$ it reduces to Eq. (33) (nonlocal regime). Thus, to determine the EDF in the general (transition) case it is necessary to solve the integral Eq. (42), which can be a quite complicated task. In practice, however, it might be more convenient to choose the appropriate probe size, which will allow application of the formula for either the collisionless or the nonlocal regime. The formulas for the transition case have been applied for determining limits of validity of theories for collisionless and nonlocal regime.[21] It was demonstrated that in unmagnetized plasma for a cylindrical probe Eq. (27) is applicable if

$$\lambda_e \geqslant \frac{3R}{4}\ln\left(\frac{\pi L}{4R}\right) \tag{44}$$

and Eq. (36) is valid for

$$\lambda_e \leqslant \frac{R}{7}\ln\left(\frac{\pi L}{4R}\right) \ll \lambda_\varepsilon. \tag{45}$$

2. Measurements of anisotropic EDF

In this case the methods for measurements of anisotropic EDF are rather well developed for a low-pressure plasma $\lambda_e \gg d \gg h$. Note that for a high-pressure plasma the degree of anisotropy is usually small. The method of measurement depends on the shape of the probe. A synopsis of the theories for a spherical probe in a plasma with anisotropic EDF[7,133,134] and for a plane (i.e., flat one-sided) probe[134,135] are given below.

In a strongly anisotropic plasma the two term expansion of the EDF given by Eq. (28) is invalid. In this case the distribution function $f(\mathbf{v})$ can be given as an expansion in spherical harmonics.[42,136] For the case of axial symmetry with axis z parallel to the directed velocity (for example, in absence of magnetic field z is parallel to electric field $\mathbf{E}$) we can represent $f(\mathbf{v})$ as $f(\varepsilon,\vartheta)$. In this case the dependence on the angle ϑ between $\mathbf{v}$ and the cylinder axis can be expanded in Legendre polynomials:

$$f(\varepsilon,\vartheta)=\sum_{j=0}^{\infty} f_j(\varepsilon)P_j(\cos\vartheta). \tag{46}$$

The physical meaning of the coefficients f_j and their connection to fluid moments can be found in Ref. 42. We can see from Eq. (46) that if all these coefficients could be measured, one could recover the entire anisotropic distribution function. However, measurement of a few of the first coefficients of the expansion yields a good approximation.

a. Flat one-sided probe. The method was developed for a plasma with axisymmetric EDF[137] but may be also extended to a plasma with arbitrary EDF.[135] The method is valid for $h \ll d$ (thin sheath) and $\lambda_e \gg d$ (collisionless case) or in the presence of weak magnetic field ($R_{Le} \gg d$). To measure f_j the following must be done. The second derivative j_e'' of the probe current with respect to the voltage (for $-eV>0$) is measured for different angles Φ_0. Here Φ_0 is an angle between the axis of plasma symmetry and the outer normal to the collecting plane of the probe. The measured $j_e''(-eV,\cos\Phi_0)$ allows coefficients f_j to be calculated. Formulas for such calculations are quite cumbersome and are provided in Refs. 135 and 137. For illustration we give here the expression for f_0

$$f_0(-eV)=-\frac{m^2}{4\pi e^3}\int_{-1}^{1} j_e''(-eV,\cos\Phi_0)d(\cos\Phi_0). \tag{47}$$

The method is valid for arbitrary degree of anisotropy of the EDF. In the case of a strongly anisotropic function the measurements for a rather large number of different angles Φ_0 can increase the accuracy of the EDF estimate. However, the accuracy of the f_j measurements is limited by the accu-

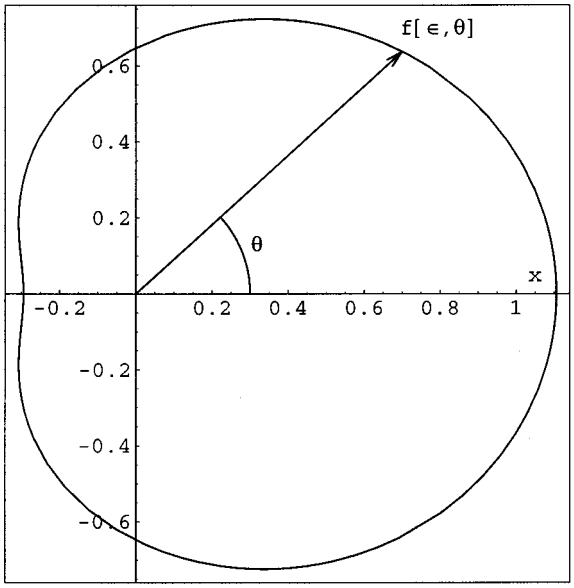

FIG. 9. Angular distribution of EDF (in arbitrary units) for electrons with energy 20 eV in a low-pressure (65 Pa) helium discharge positive column for discharge current equal to 0.5 A. The plasma symmetry axis coincides with x axis.

racy of the experiment and becomes more inaccurate for higher values of the index j. In Ref. 137 the optimal number of angles and an upper practical limit on index j were estimated.

This method has been applied for measurements of the drift velocity as a function of electron energy in noble gas plasma discharges[138] and for studies of the momentum relaxation of electron fluxes.[139] Investigations of momentum relaxation can provide differential cross sections of electron atomic (molecule) collisions (see Sec. V A for details). Application of the method has also provided EDF measurements in noble-gas short length discharges[140–142] and in hollow cathode arcs.[143]

Studies of EDF anisotropy in a magnetized plasma were performed in Refs. 22, 144. In Ref. 22 deviation of the EDF from spherical symmetry was found only for low energy (<4 eV) electrons. However, the Larmor radius of these electrons is smaller than the probe dimension, hence the application of the model might not be valid. The diffusion of low energy electrons to the probe could cause apparent anisotropy of the EDF for this energy range.

Figure 9 demonstrates angular distribution of the EDF (in arbitrary units) for electron energy 20 eV.[145] The measurements were conducted in a low-pressure (65 Pa) helium discharge positive column for discharge current equal to 0.5 A.[138] The vacuum vessel was a glass hot cathode discharge tube of diameter 3 cm and length 40 cm. In the figure, the plasma symmetry axis coincides with the x axis.

b. Spherical probe. For the case $h \ll R$ a spherical probe measures the EDF in speed or in energy (the coefficient f_0) in a plasma with arbitrary-symmetry EDF. An approach similar to that in the previous paragraph yields an analog of Druyvesteyn's equation[64]

$$f_0(-eV) = -\frac{m^2}{8\pi^2 R^2 e^3}\,\frac{d^2 I_e}{dV^2}. \tag{48}$$

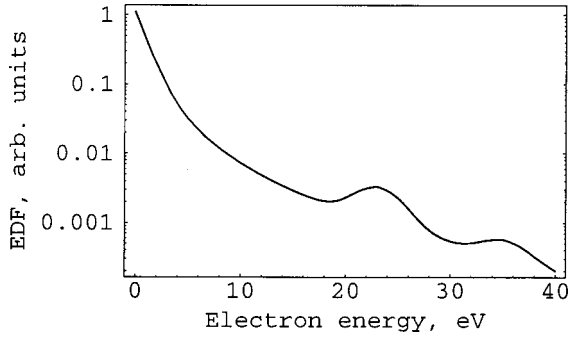

FIG. 10. EDF in a low-pressure (13 Pa) hydrogen constricted arc plasma at the discharge axis.

If the condition $h \ll R$ is not fulfilled, Eq. (48) is only valid for a spherically symmetric probe sheath.[7,146] This is true, for instance, in a plasma which has isotropic EDF for all electrons with exception of a low density high energy tail.

This method has been applied to constricted discharges.[146,147] Figure 10 presents the EDF in energy space in a low-pressure (13 Pa) hydrogen constricted arc discharge. Two peaks of the EDF corresponding to energy of 22 and 35 eV are due to electrons accelerated by the electric field in the constricted region of the plasma.

B. Measurements of IDF

Measurements of the IDF in a plasma are more complicated than the measurements of the EDF. The ion probe current (and its derivatives) for appropriate probe potentials is usually much smaller than the electron current (and its derivatives). This is caused by the large difference between the electron and ion mass ($m_e/m_i \ll 1$) and their mean-free paths ($\lambda_i < \lambda_e$). Therefore, in general, it is difficult to extract the ion current from the total probe current. Furthermore, the measurement of the IDF, $F(\varepsilon)$, is possible only for much lower gas pressure than that for the EDF, since all methods are based on an analog of the Druyvesteyn Eq. (27):

$$F(|eV|) = \frac{m_i^2}{2\pi e^3}\left|\frac{d^2 j_i}{dV^2}\right|, \tag{49}$$

which requires that $\lambda_i \gg d+h$. We emphasize again that there is no nonlocal regime for ions. Nevertheless, IDF measurements are possible in particular cases for which the second derivative of electron current j_e'' is suppressed in the ion retardation region of the characteristic. We consider a few of these cases below.

1. Plasma with negative ions

Measurements of the IDF for negative ions by using Eq. (49) have been carried out, for instance, in Ref. 148, and results of such measurements have been reviewed in Ref. 149. Figure 11 illustrates typical results of the measurements.[149] Note that for low energies (<0.1 eV) the errors might be significant, for example due to finite conductivity of the plasma, and cause false additional peaks on the IDF or EDF.[150]

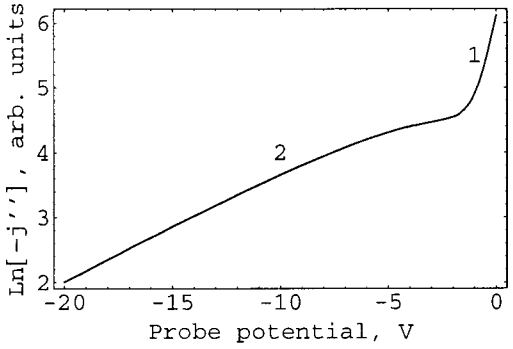

FIG. 11. Typical result of measurements of $\ln(-j'')$ in a SF_6/Ar plasma with negative ions. Curve (1) corresponds to ions with $T_i=0.5$ eV and curve (2) to electrons with $T_e=5$ eV.

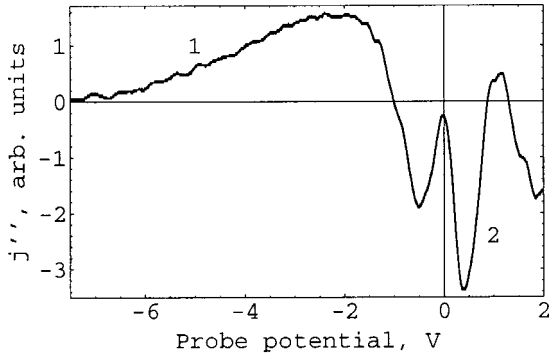

FIG. 13. Typical result of measurements of j'' in a magnetized helium ($p=0.4$ Pa, $B=0.01$ T) plasma. Curve (2) corresponds to ions with $T_i=0.1$ eV and curve (1) to electrons with $T_e=1$ eV. After Ref. 158.

2. Electronless plasma

Such plasma can arise, for example, in afterglow of electronegative gas discharges.[151,152] Results of measurements of the IDF for positive and negative ions in the plasma are given in Refs. 152 and 153. However, the accuracy of the measurements cannot be high, as it is difficult to separate currents of positive and negative ions from each other (both currents are of the same magnitude).

3. Magnetized plasma

As we have seen in Sec. II A, the electron current is strongly suppressed in a magnetized plasma. The ion current is affected significantly less by the magnetic field since $R_{Li} \gg R_{Le}$. Moreover, the ratio between electron and ion currents depends on the probe orientation with respect to the magnetic field, which creates a possibility to separate the currents or their derivatives and, thus, to measure the IDF. For this purpose, different constructions have been developed[23,154–156] utilizing electric or magnetic fields and special probe designs. The discussion of these and other probe constructions can be found in Sec. IV B. As a rule these methods cannot provide detailed IDF measurements but rather estimates of T_i.

A probe proposed in Ref. 156 has been modified in Ref. 157 into a plug probe for IDF measurements. It consists of a cylindrical rod with insulating end plugs (Fig. 12), and is operated by obtaining the current-voltage characteristic and its first and second derivatives for different orientations of the rod with respect to the magnetic field. The plugs prevent electrons reaching the ends of the probe. When the rod is oriented parallel to the magnetic field, the electron current is significantly reduced, so that the ion current becomes dominant. If $R_{Li} \gg L$, the IDF can then be measured. For perpendicular orientation the probe works practically as a usual Langmuir probe, as the area of the covered end surface is much less than the total probe area. In that case the EDF can be measured. By rotating the probe gradually from parallel to perpendicular one observes that the electron part of the characteristic increases, while the ion part remains unchanged. This clearly demonstrates how one can separate the ion current from the electron current.

A typical result of measurements of j'' by a plug probe is presented in Fig. 13.[158] The measurements were carried out in the simple magnetized torus "Blaamann"[35] with helium pressure 0.4 Pa and magnetic field 0.01 T, corresponding to $R_{Li}=13$ mm for $\varepsilon_i=0.2$ eV. A molybdenum probe with radius 0.125 mm and length 4 mm was used. The radius of the ceramic end plugs was 0.5 mm.

With some modification the plug probe could also be used to measure the IDF in an unmagnetized low-pressure plasma, for instance by constructing a probe arrangement that produces its own local magnetic field. The size of the entire construction should be less then λ_i for application of Eq. (49).

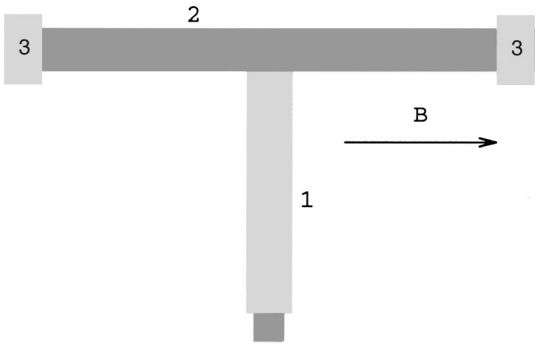

FIG. 12. Sketch of the plug probe. Ceramic layer (1), molybdenum wire (2), and ceramic insulating plug (3).

C. Details of EDF and IDF measurements

We have seen that reconstruction of the EDF or IDF requires measurement of electron probe-current I_e, ion probe-current I_i or their derivatives with respect to probe potential V. In most studies of distribution functions one makes use of the Druyvesteyn formula, hence $I''=d^2I/dV^2$ is measured. There are several methods for obtaining I'', among these are probe-current modulation, differentiating amplifiers, and analog numerical differentiation. Naturally, the same methods can be applied for the determination of first derivative I'. A combination of these methods is also possible. Numerical differentiation with additional smoothing may also be applied.[159,160]

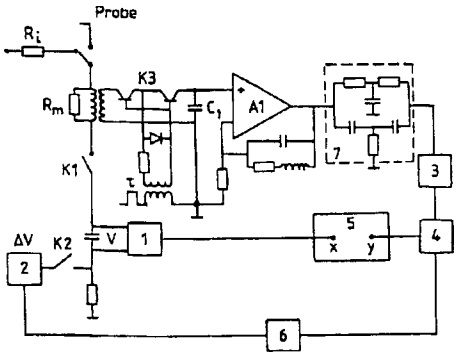

FIG. 14. Block-diagram for a probe-current modulation method. The schematic shows the electronics for the opamp circuit with tuning at the frequency 2Ω. Using a diode as a simulation for the plasma the circuit had an accuracy in calculating d^2I/dV^2 of a few percent. After Ref. 21.

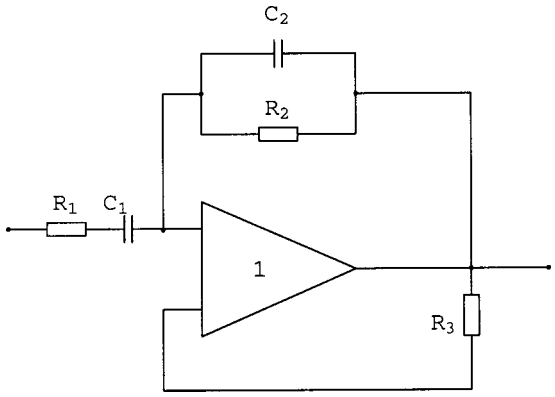

FIG. 15. A bandwidth limited differentiating network.

1. Probe-current modulation methods

Probe-current modulation methods have been extensively applied in the past.[5–9,11,17,21,24] They allow measurements to be conducted in stationary plasma and in plasma with periodically changing properties.

In these methods a small amplitude alternating voltage ΔV (modulating signal) super-imposed on the steady bias probe potential V is applied to the probe and a given harmonic of the probe current is measured. If the amplitude of the modulating signal is sufficiently small, the magnitude of the harmonic component is proportional to I' or I''. In practice, two forms of the modulating signals have been widely applied:

$$\Delta V_1 = 2U_1 \cos \Omega t \tag{50}$$

and

$$\Delta V_2 = \sqrt{2}U_2(1+\sin \Omega_1 t)\sin \Omega_2 t, \tag{51}$$

where $\Omega_2 \gg \Omega_1$.[161–163] For the first signal, expanding the probe current

$$I(V+2U_1\cos \Omega t) = [I(V)+U_1^2 I''(V)+\cdots]+[2U_1 I'+U_1^3 I'''+\cdots] \times \cos \Omega t + \left[U_1^2 I'' + \frac{1}{3}U_1^4 I'''' + \cdots\right]\cos 2\Omega t + \cdots \tag{52}$$

and retaining only the leading term for each harmonic, we can see that the magnitude of the frequency component Ω is proportional to I', and that on frequency 2Ω is proportional to I''. Similarly it can be shown that for the second signal the magnitude of the harmonic on frequency Ω_1 is proportional to I''. In the general case, the measured I' or I'' are the convolutions of the real I' or I'' and instrumental functions (see Sec. II C).

Figure 14 represents a possible block diagram for the method.[21] Block 1 gives the smooth ramp-up of the probe potential V. The switch $K1$ connects the probe to the measurement circuit, and is closed for duration t longer than the duration τ_i of the measurement. The modulating signal in Eq. (50) is created by block 2. The switch $K2$ applies the modulating signal to the probe during a time interval t_m, where $\tau_i < t_m < t$. This attenuates the transient processes in the probe circuit and reduces noise. The measuring system consists of a measuring resistor R_m, a switch $K3$ (which is closed for the duration of measurements τ_i), an integrating capacitor C_1, an amplifier $A1$ with high input resistance, and a resonance feedback circuit at the frequency 2Ω, filter 7 for suppressing of the frequency Ω, narrow-band amplifier 3 at the frequency 2Ω, phase detector 4 (or equivalently, lock-in amplifier), and measuring device 5. Block 6 generates the frequency 2Ω and the system registers this frequency. Resistor R_i calibrates the measuring device.

2. Analog numerical differentiation

Numerical differentiation is based on the finite difference schemes

$$I' = [I(V+\Delta V)-I(V)]/\Delta V \tag{53}$$

and

$$I'' = [I(V+\Delta V)+I(V-\Delta V)-2I(V)]/\Delta V^2 \tag{54}$$

or some more sophisticated schemes.[136] Discussion of various circuits for numerical differentiation can be found in Refs. 21, 164, and 165.

3. Differential amplifiers

The method is based on the use of a differential circuit. The probe is swept linearly in time and $dI/dV \sim dI/dt$. A typical network is presented in Fig. 15. To cutoff the high frequency components and to reduce noise a limitation in bandwidth is required. This is done by introducing additional elements R_2 and C_2 in a standard differentiating circuit.[17] Details of the method can be found in Ref. 17 and references therein. This method allows fast measurements in nonstationary plasmas.

4. Measurements of distribution functions

In measurements of EDF or IDF the following steps should be taken.

(1) For given experimental conditions it is necessary to choose appropriate size and orientation (in magnetized plasmas) of the probe in order to ensure that the probe operates in one of the regimes described in Sec. III A.

(2) The measurements of I' for the nonlocal case and I'' for the collisionless case should be performed, for instance, by one of the methods described above.

(3) The plasma potential should be determined. Methods for such measurements are different for collisionless and nonlocal regimes and described in detail in Sec. IV D.

(4) For a given plasma potential, it is possible to recover the distribution function by applying the appropriate formula of Sec. III A.

IV. MEASUREMENT OF FLUID OBSERVABLES

This section deals with methods for measurements of fluid observables defined as statistical moments of the velocity distribution function. This includes electron number density n, electron and ion fluid velocity $\mathbf{u}_{e,i}$, and electron and ion temperature $T_{e,i}=2/3\langle\varepsilon\rangle$, where $\langle\varepsilon\rangle$ is the mean particle kinetic energy. In the fluid equations these observables appear as time-dependent fields in configuration space, along with the electromagnetic fields. For this reason the electrostatic field (or rather the electric plasma potential ϕ) will be treated as a fluid observable in this section. If high frequency magnetic fields play an important role in the phenomena observed, electric probes should be applied with care.

The measurement of fluid velocity constitutes a particular problem. The direct measurement of the anisotropic part of the velocity distribution function is generally very complicated, and can seldom be performed in practice (see Sec. III A 2). Simpler methods exist, like the so-called Mach probe. This, and a few other methods are briefly discussed in Sec. IV F.

A. Electron temperature

We start by determining the electron temperature from the single probe characteristic. We shall consider three regimes of probe operation in accordance with Sec. II.

In the *collisionless regime*, the EDF can be recovered by applying the Druyvesteyn Eq. (27) if it is isotropic, or by methods mentioned in Sec. III for the anisotropic function. In both cases we can define $\langle\varepsilon\rangle$ and thus T_e as an integral over the distribution function.

If the EDF is Maxwellian the electron current has exponential behavior for repulsive potentials and thus $\mathcal{I}_e(V)=\ln I_e(V)$ is a linear function (Fig. 16). In this case T_e can easily be found from the slope of the linear part as

$$T_e = e\frac{dV}{d\mathcal{I}_e}. \tag{55}$$

Since we measure the total current $I=I_e+I_i$, the ion component I_i should be subtracted from I to obtain the EDF. The influence of ion current is discussed in Sec. II. Often $I_i^{\mathrm{sat}} \ll I_e^{\mathrm{sat}}$ and the ion current is crudely approximated as a linear function in the transition region. Another method to take into account the ion current is to measure the first or second derivatives of the total current with respect to the probe potential. Slow change of I_i in the transition region allows one to extend the energy interval where influence of ion current can be neglected.

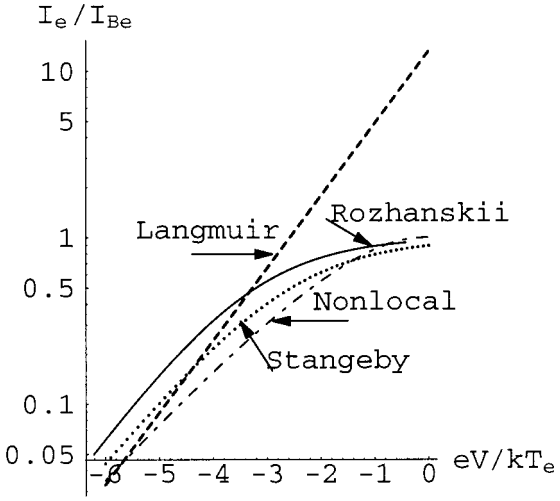

FIG. 16. Semilog plot of electron current given by Langmuir formula and diffusive (nonlocal [Eq. (37)], Rozhanskii [Eq. (19)], Stangeby Refs. 16 and 78) models. Current is normalized by Bohm electron saturation current I_e^{sat}. All curves are calculated for the same plasma parameters with classical diffusion coefficient.

In the *nonlocal regime*, we also can obtain the EDF and thus determine T_e as $\langle\varepsilon\rangle$. According to the expressions derived from kinetic theory, increasing pressure [Eq. (35)] or magnetic field [Eq. (37)] makes the electron current grow more slowly with V than exponential, in particular near the plasma potential. Figure 16 shows the deviation from the straight line (Langmuir case) of the semilog plot of electron current given by the nonlocal model [Eq. (37)]. It is seen that for high negative potentials ($V<-3T_e/e$, i.e., around the floating potential) $\ln I_e(V)$ does behave like a straight line but with a smaller slope than that in the Langmuir case. The application of Eq. (55) to this region can yield T_e overestimated up to 30%. For larger negative potentials the ion component becomes important and starts to contribute to errors in T_e measurements.

We find a similar situation in the *hydrodynamic regime*, since most of probe models for this regime are diffusive. The typical diffusive model [by Rozhanskii, Eq. (19)] for weakly ionized magnetized plasma is chosen to demonstrate the deviation of electron current from the exponential behavior. Again, we can see in Fig. 16 that the deviation of the slope from the Langmuir case is less for large negative potentials and the model shows a straight line parallel to the one given by the nonlocal model for these potentials. Thus, also in this regime T_e obtained from applying Eq. (55) to this region can be overestimated up to 30%. It is argued in Refs. 44, 166, and 167 that the model predicts linear behavior of the characteristic in the transition region (corresponding to $-3T_e/e<V<0$ in Fig. 16) and T_e can be found then with higher accuracy than from Eq. (55). As an illustration, the electron current from the diffusive model for fully ionized magnetized plasma by Stangeby[16,78] (with classical diffusion coefficient) is also presented in the same figure, showing a behavior similar to the models discussed above.

Since all models provide expressions for the electron current (corrected for the ion contribution), they can be fit to the experimental characteristic to yield correct T_e. In prin-

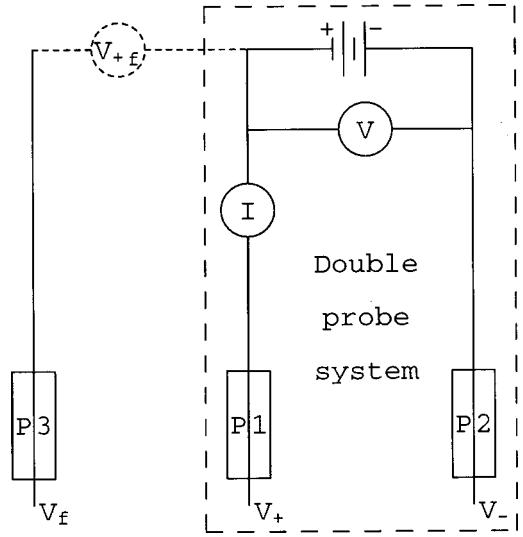

FIG. 17. Sketch of the double system ($P1$ and $P2$, inside the dashed contour) and independently floating probe $P3$. V_{+f} measures the $P3$ to $P1$ potential. All probes yield the triple probe system.

ciple, such a fit can provide T_e, T_i, and n_e. In practice, however, to extract the ion temperature can be very problematic, and some *a priori* information about T_i is often required.

In fluctuating plasma the *double probe*[168] might be very useful for measurements of the electron temperature. It consists of two probes biased with respect to each other (V is swept) but insulated from ground so the entire system floats (see Fig. 17). The advantage of such probe is that it does not require a reference electrode and, therefore, can be applied in the electrode-less plasmas like rf or space plasmas. In the limit $S_p^{(1)} \gg S_p^{(2)}$, where $S_p^{(1)}$ and $S_p^{(2)}$ are probe areas, the double probe is equivalent to the single probe. Here we shall consider the case when $S_p^{(1)}$ does not differ much from $S_p^{(2)}$. A schematic of the potential distribution between the probes is shown in Fig. 18 (for a given V). Since the system floats, both probes are negative with respect to plasma potential in order to prevent a net electron current. The typical characteristic is presented in Fig. 19. From this figure we can see that the total current to the system can never be greater than ion saturation current, since any electron current must be balanced by an ion current. That has the advantage of minimizing the disturbance of the plasma and the power flux to the probe. However, the fact that the probe collects electrons

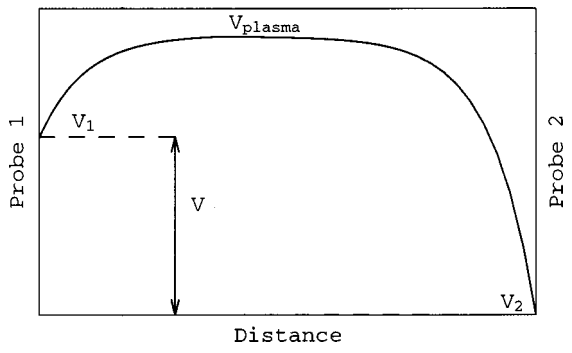

FIG. 18. Schematic of the potential distribution between probes $P1$ and $P2$.

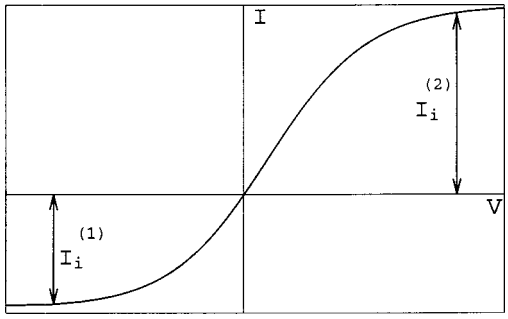

FIG. 19. Typical characteristic of double probe with different tips area ($S_p^{(2)} > S_p^{(1)}$).

only from the tail of the EDF, without sampling the bulk distribution, affects the accuracy of the T_e measurements. Following Ref. 6 we consider here only the theory for the double probe in the case when both tips are operated in the collisionless regime. Defining $I_i^{(1)}$, $I_e^{(1)}$, $I_i^{(2)}$, and $I_e^{(2)}$ as the ion and electron currents to the probes 1 and 2 (all are defined with positive sign), we have the condition of the floating system $I_i^{(1)} + I_i^{(2)} - I_e^{(1)} - I_e^{(2)} = 0$ and the current in the loop (total current) $I = I_e^{(1)} - I_i^{(1)} = I_i^{(2)} - I_e^{(2)}$. Applying the latter equation along with the Langmuir formula Eq. (26) for the electron current to both probes, we end up with the expression

$$\left[\frac{dI}{dV}\right]_{V=0} = \frac{e}{T_e} \frac{I_i^{(1)} \cdot I_i^{(2)}}{(I_i^{(1)} + I_i^{(2)})}. \tag{56}$$

Here, $I_i^{(1)}$ and $I_i^{(2)}$ are assumed to be independent of V, i.e., both probes are negative enough to collect the ion saturation currents. From Eq. (56) T_e can be obtained from the slope at $V=0$ and the measured magnitudes of $I_i^{(1)}$ and $I_i^{(2)}$. The derivation was simplified by assuming the ion current to be independent of voltage, which is the case only if the probe sheath is thin. Determination of T_e for realistic sheaths, i.e., for the case when I_i is a function of V, was considered in Ref. 9. The effect of ion collisions was taken into account in,[169] where it was shown that for $\lambda_i / d \to 0$ the errors do not exceed 15%. Even though Eq. (56) was derived from the Langmuir formula, the only relevant feature of that formula is the exponential behavior of the electron current for V around the floating potential. Since the diffusive theories give a similar current behavior in this potential range, but with apparent T_e overestimated by approximately 30% (see Fig. 16), the error of applying Eq. (56) in regimes where the diffusive theories are appropriate, should be of this order. Of course, similar derivations as that leading to Eq. (56) could be made for the double probe in the diffusive regime by application of the appropriate models for the probe characteristic.

A swept double probe technique first described in Ref. 170 can be used for temperature fluctuation measurements. The technique is based on a fit of the measured root-mean-square of current fluctuations as a function of voltage across two identical probe tips to a six-parameter model for the current fluctuations.[171,172]

A *triple probe* permitting instantaneous T_e measurements was proposed in Ref. 173. This technique requires the

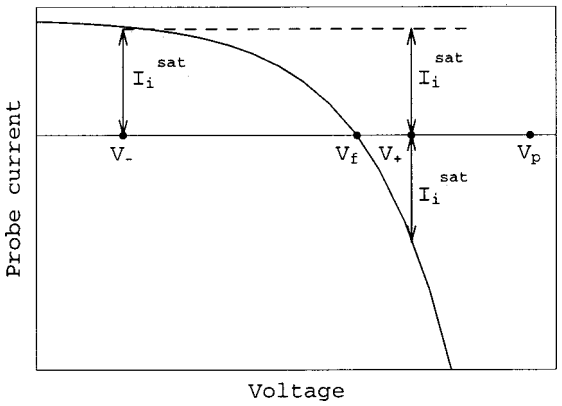

FIG. 20. Part of probe characteristic for potentials below the plasma potential V_p with three points (V_-, V_f, and V_+) utilized in the triple probe method.

floating double probe system $(P1, P2)$ and one probe $(P3)$ floating independently (Fig. 17). All probes are identical and the double probe system is biased negatively enough to collect the ion saturation current. Such a system provides three points on the I-V characteristic (Fig. 20) from which T_e can be obtained by

$$T_e \approx e(V_+ - V_f)/\ln 2. \tag{57}$$

Here, V_f and V_+ are potentials of floating and positively biased probes, respectively. The fact that this method does not require sweeping of the probe potentials, and almost no data processing, has made it widely used for T_e fluctuation measurements. The accuracy of this method can be affected by various factors. In derivation of Eq. (57) it was assumed that the areas of the probe tips are equal, that the ion current is independent of probe potential, and that there are no gradients in plasma potential, electron temperature, and density arising due to the spatial separation of the tips. Violation of any of these assumptions introduces error. Estimates of such errors are provided in Refs. 173–175. In Ref. 174 the effect of ion current and ion temperature is considered for the case of a collisionless plasma in the orbital motion limit. In Ref. 175, it is demonstrated that a significant plasma potential gradient might give rise to negative temperature. The sensitivity of the method to inhomogeneities in the plasma also leads to phase delay and decorrelation effects. In a magnetized plasma the effect of shadowing can also destroy the measurements. Some solutions for these problems have been suggested in Refs. 175–180.

If the sweep time τ_{sw} is much shorter than the typical fluctuation time scale $\tau_{sw} \ll \tau_{fl}$, it is possible to obtain ''instantaneous'' values of density, electron temperature, and plasma potential from the characteristic of a single probe.[181–185] The method is very attractive for experimentalists since all information is acquired from a single probe and thus all problems arising from the spatial separation of the tips are avoided. Since a finite time τ is required for the charge carriers to acquire their equilibrium distribution,[9] the probe cannot be swept faster than this time. If this condition is not satisfied, different dynamic effects on the probe characteristic start to play a role, for example, the displacement,[9,186] polarization[187,188] and stray capacitive currents.[184] Often, the critical sweep frequency can be estimated and contributions from these currents can be avoided by sweeping at lower frequencies. The problem of stray capacitance can be solved, for instance, by using a reference probe outside the plasma.[184,189]

When applying a fast sweep probe in magnetized plasma and the probe is in the hydrodynamic regime (the same is valid for high pressure plasma), electrons diffuse to the probe and the stationary density profile is established on a time scale $\tau = \Lambda^2/D$.[44] Here Λ is a diffusion length and D is diffusion coefficient. We can then obtain an upper limit on the sweep frequency from the estimate

$$\tau = \frac{a^2}{8D_\perp} = \frac{a^2\omega_e^2}{8\nu_e^2 D_\parallel} = \frac{3a^2\omega_e^2}{8v^2\nu_e} \tag{58}$$

(Ref. 44), where $D_\perp$ and $D_\parallel$ are classical diffusion coefficients perpendicular and parallel to the magnetic field, respectively. Thus, time sweep must be chosen to satisfy both conditions $eV_{sw}\tau/T_e \ll \tau_{sw} \ll \tau_{fl}$ simultaneously. Here, V_{sw} is the voltage range of the sweep.

The generation of harmonics of the driving frequency due to nonlinearity of the probe characteristic can serve as a diagnostic tool.[190] The method is sometimes called *the harmonic technique* and has been applied in number of investigations.[190–192] The basis of the technique is as follows. A sinusoidal voltage sweep, $V_1 \sin \omega t$, with the amplitude V_1 is substituted into the Langmuir expression for electron current. The mean probe voltage is kept close to the floating potential. For these potentials the ion current is assumed to be independent of probe voltage. Taking into account that the periodic exponential term can be written in terms of modified Bessel functions $I_n(z)$ of integer order n:

$$e^{x\cos\omega t} = I_0(x) + 2\sum_{n=1}^{\infty} I_n(x)\cos(n\omega t), \tag{59}$$

it is easy to show[190–192] that the ac component of the total current will be proportional to the second term of Eq. (59), where $x = eV_1/T_e$. The dc current arising from the first term of that equation is called the sheath rectification current. The evaluation of T_e is possible from the ratio of any two measured harmonics of the current oscillations since the V_1 is known. An analysis of Taylor expanded Bessel functions made in Refs. 191 and 192 demonstrated that T_e can be obtained from the ratio of the first two harmonics as

$$T_e = \frac{eV_1}{4}\,\frac{I_1}{I_2} \tag{60}$$

with error of about 1% for $eV_1/T_e = 0.5$ and 5% for $eV_1 = T_e$. To resolve the time variations of the electron temperature the ac signal must have high frequency, hence the above discussion of the limitations of the sweep frequency remains relevant also for the harmonic method. Probe theories for magnetized plasma[16,44] might require a more complicated analysis for estimating T_e.

Temperature fluctuations can also be found from the floating potential generally given by $V_f = V_p - \mu T_e/e + V_0$, where μ and V_0 are assumed to be constants. Conventionally, the position of V_f with respect to V_p is calculated as-

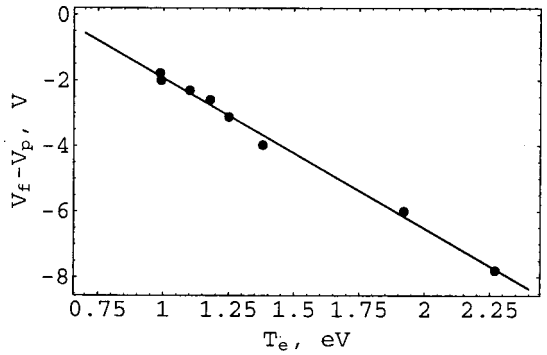

FIG. 21. Experimental measurements of μ for cylindrical Molybdenum probe with $R=0.25$ and $L=5$ mm oriented perpendicular to the magnetic field $B=0.15$ T. Plasma parameters are helium pressure $p=0.3$ Pa, the typical plasma density is $n\sim 3\times 10^{17}$ m^3 and the ion temperature $T_i\approx 0.2$ eV. The coefficients $\mu=4.6\pm 0.2$ and $V_0=(2.6\pm 0.2)$ V are obtained from fitting the data (dots) to a linear function (full line). Measurements have been conducted in a simple magnetized torus Ref. 35.

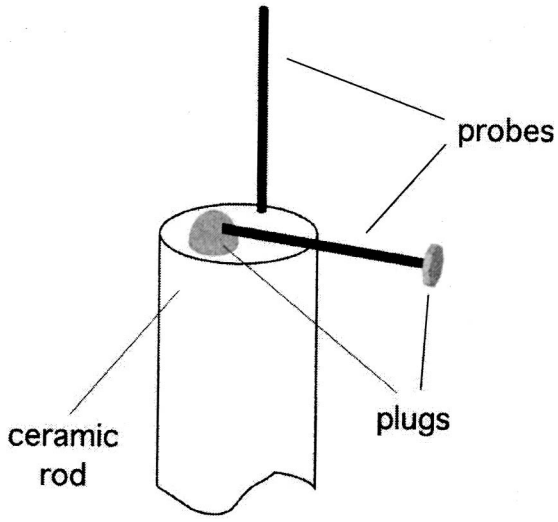

FIG. 22. Sketch of probe system. After Ref. 193.

suming random current with acoustic velocity for ions and Langmuir formula for electrons, and in this case $V_0=0$. In magnetized plasma, however, the current ratio, and, therefore, μ and V_0, depend on the magnetic field strength and the probe size and orientation. The validity of this formula can be verified and μ and V_0 can be determined experimentally for given plasma conditions. To do so one can measure time averaged $V_f - V_p$ as a function of averaged T_e in various locations in the plasma with different electron temperature. The coefficients μ and V_0 are then obtained by fitting the data to a linear function. An example of such measurements is presented in Fig. 21. The same can be done if an analytical model of the probe characteristic is available for the given experimental conditions. The fluctuating part of T_e is given as

$$\tilde{T}_e = e\,\frac{\tilde{V}_p - \tilde{V}_f}{\mu}. \tag{61}$$

Note that inaccuracies in μ only affect the amplitude of $\tilde{T}_e$ but not its spectral characteristics and phase. Independent measurements of the time averaged plasma potential V_p and its fluctuations $\tilde{V}_p$ can be provided by probes described in the next section; ion sensitive probes, emissive probes, and others. In Refs. 193 and 194 a plug probe was utilized for measuring plasma potential fluctuations. To obtain greater difference between the signals from the probe measuring the plasma potential and the probe measuring floating potential, and thus more accurate $\tilde{T}_e$ measurement, the latter was oriented perpendicular to the magnetic field (see Fig. 22). In general, any pair of probes, for example, one parallel and one perpendicular to the magnetic field, can be used to find $\tilde{T}_e$ without measuring $\tilde{V}_p$. By applying Eq. (61) to the two probes we find

$$\tilde{T}_e = e\,\frac{\tilde{V}_{f1} - \tilde{V}_{f2}}{\mu_2 - \mu_1}, \tag{62}$$

assuming that the $\tilde{T}_e$ and $\tilde{V}_p$ are the same at the two probe positions. Thus the probes will have to be located very close to each other. There are some advantages of this method compared with the triple probe technique. We only need two probes, and shadowing effects are more easily avoided if one probe is perpendicular and another is parallel. More importantly, perhaps, the method does not depend on the validity of a particular probe theory, i.e., errors connected with the invalid application of the Langmuir formula, lack of ion current saturation, and other sources of error described above are avoided.

B. Ion temperature

As discussed above, it is quite complicated in general to extract information about the ion current from the total current. This is possible only in particular cases when the electron current can be reduced to a level comparable to the ion current, and thus create an *ion sensitive probe*. This could be done for instance by application of an imposed electric field to repel electrons, by an imposed magnetic field or a magnetic field already present in the plasma, or by employing partly insulated probes.

Below we describe some probe constructions whose operation is based on the model for a probe in collisionless regime, or more precisely, on the Langmuir formula [Eqs. (25) and (26)] for ions. Thus, T_i can be found by the same methods used to recover T_e [see Eq. (55)]. Conditions for the collisionless regime were discussed in Sec. II. If the probe construction does not satisfy these conditions, the effect of diffusion of ions to the probe might give errors and should be investigated separately. If ions are in the diffusive regime[44,75] then, according to Eq. (18) the ion current depends on both T_e and T_i (see also Fig. 28 described in Sec. IV D). If $T_e \gg T_i$ the slope of the characteristic can be dominated by T_e and make it impossible to extract T_i.

Retarding field ion energy analyzers are widely used and consist of a number of grids and a current collector.[19,195–199] Positively biased grids repel ions and then the collector operation can be described by models for a conventional probe, provided effects of the biased grids on electrons can be neglected. If this is the case, the Langmuir formula [Eq. (25)] for a flat one sided probe takes the form

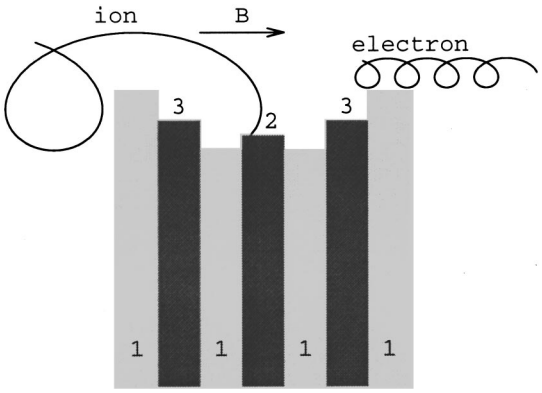

FIG. 23. Sketch of Katsumata probe. Insulation (1), central electrode (2), and guard electrode (3).

$$I_i \sim \int_{\sqrt{2eV_{gr}/m_i}}^{\infty} v_{\parallel} F(v_{\parallel}) dv_{\parallel}, \tag{63}$$

where V_{gr} is the voltage on the ion repeller grid, and $v_{\parallel}$ is the component of the velocity perpendicular to the collector surface. Assuming a Maxwellian distribution the ion temperature can be extracted from $I-V$ characteristic by applying an equation similar to Eq. (55). In the presence of a magnetic field the collector surface is oriented perpendicular to the magnetic field, and then the temperature corresponding to the ion motion parallel to the magnetic field is measured. The analyzer itself can disturb the ambient plasma and the IDF as it creates a shadow along the magnetic field. In Ref. 200 the study of such perturbations based on a kinetic model proposed in Ref. 201 was carried out. It was demonstrated that the standard procedure of extracting T_i from the $I-V$ characteristic might yield significant errors and new analysis methods allowing extraction of T_i from the unperturbed plasma was suggested. Some particular analyzer designs, for example, with capillary plate[202] or with coaxial cylindrical electrodes[203] are argued to provide perpendicular ion energy. In Ref. 204 one can find details on application of analyzers in low-pressure radio frequency discharges and a comprehensive reference list.

In a magnetized plasma the *Katsumata probe*,[155,205] which is a probe with a cavity (Fig. 23), can provide estimates of the characteristic perpendicular ion energy. The electrons cannot reach the probe due to their small gyroradius and the ions are repelled by a positively biased electrode inside the cavity. The probe has a complicated geometry in the magnetic field, which makes theoretical description of sheaths and current collection quite cumbersome.[19] Some attempts of numerical simulations[206,207] of the Katsumata probe are available. In Refs. 208 and 209 a simplified version of the probe was proposed and applied for both hot ($T_i \sim 100$ eV)[208] and cold ($T_i \sim 0.1$ eV)[209] ions.

The *plug probe*, described in Sec. III B, can be used to measure the IDF when in a collisionless regime.

In the presence of a strong magnetic field ($R_{Le} \gg R$), the electron current can be reduced sufficiently to detect the ion component by a conventional cylindrical probe oriented parallel to the magnetic field.[210] Different collecting areas for electron and ion current (end and side surfaces, respectively) yield significant reduction of the ratio I_e/I_i. For such measurements a long ($R \ll L$) cylindrical probe with a holder perpendicular to both probe and magnetic field is advisable.

A probe employing an imposed magnetic field was suggested in Ref. 211. The difference from the probes described above is that it can be applied in an unmagnetized plasma. The probe was proposed for detection of negative ions and consists of a positively biased orifice, with magnets behind it, and a positively biased collector. The magnets or magnetic coils provide a uniform magnetic field, which deflects electrons so that only negative ions can reach a collector. The theoretical description of such a probe along with a discussion of the design can be found in Ref. 154.

Some other techniques for ion diagnostics applied to tokamak plasmas can be found in Matthew's review.[19] An application of bolometers for such purposes has been described in Refs. 212 and 213. Double probes have been used in magnetized plasma for ion temperature measurements in Ref. 214.

C. Plasma density

It was mentioned in Sec. II B that application of probe theories outside the domain of their validity may yield significant errors in the electron density measurements. Here we discuss the techniques pertaining to such measurements, assuming that the correct model is chosen.

Plasma electron, n_e, or ion, n_i, density can be found from the electron or ion saturation current, respectively. To extract the density from the measured currents requires application of the appropriate theory for attracted charged particles. The expressions connecting ion or electron saturation current with densities, require knowledge about ion and/or electron temperatures. The temperatures T_i and T_e can be found independently from the transition part of the characteristic according to the discussion of Secs. IV A and IV B. Depending on the regime, the saturation currents may, or may not, depend on the probe voltage. In practice, it is very often assumed that for sufficiently high probe voltage the saturation current is voltage independent. If such an assumption is justified, for time resolved measurements of the density, it can be sufficient just to bias the probe to a large constant voltage without sweeping. That allows simple measurements of density fluctuations provided that T_e (and T_i if required) fluctuations are known. The latter is an important issue often neglected, since it is argued that the influence of T_e fluctuation is weak. That might not always be true, however. For instance in weakly ionized magnetized plasma both electron and ion saturation currents can depend strongly on T_e [see Eqs. (16) and (15)]. Moreover, even small amplitude T_e fluctuations might strongly influence the phase of the current oscillations, and consequently give rise to considerable phase errors for the density fluctuations. Small inaccuracies in phase of the density fluctuations may yield significant errors in the anomalous particle flux measurements [see Sec. V A]. Therefore, for correct measurements of the density fluctuations from the saturation currents, it is advisable to apply a probe cluster in order to provide $\tilde{T}_e$ measurements simultaneous with $\tilde{I}^{\mathrm{sat}}$.

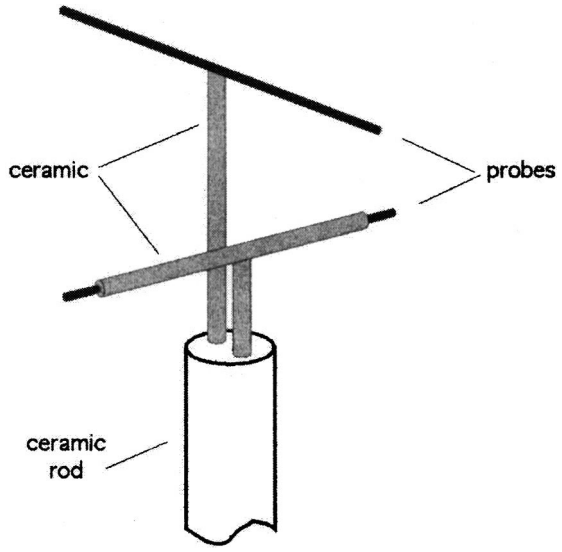

FIG. 24. Sketch of probe system. Coated probe (lower) aligned along magnetic field and conventional cylindrical probe (upper) oriented perpendicular to the magnetic field. After Ref. 84.

The cluster is not needed if time resolved density measurements are carried out by means of the fast swept probe. In this case electron temperature information can be obtained from the same characteristic. The density can be found from the saturation current if the entire characteristic is available. Otherwise, the transition part of the characteristic can also be used. In this case a suitable model for the repelled electrons should be fitted to the experimental data under assumption of, for instance, a Maxwellian distribution. An example of such a fit for electrons in the nonlocal regime and determination of n_e can be found in Ref. 35.

If measurements of the EDF or IDF are possible, n_e or n_i can be found as an integral over the distribution function. The accuracy of such a method is higher than that of the previous one since no *a priori* information about the shape of the distribution is required. The method can also provide the density of negative ions[149] if such ions are abundant.

Based on this discussion for single probe measurements we can briefly describe the utility of some other techniques. The double probe collecting mostly ions can only provide ion density measurements. One of the tips biased negatively in the triple probe can also be used. Simultaneous measurements of T_e fluctuations can be used for correction of the density fluctuations. Difficulties in the theoretical description of ion current collection by ion sensitive probes might prevent their application to ion density measurements.

The spatial resolution of probe measurements in magnetized plasma depends on the orientation of the probe with respect to the magnetic field. Probes aligned along the magnetic field provide higher spatial resolution than those oriented perpendicular. Nevertheless, small errors in alignment of parallel probes can cause significant errors in the current measurements. In comparison with the conventional parallel probe, the *coated probe*,[84] shown in Fig. 24, is 7–10 times less sensitive to alignment errors. The electron density can be obtained from the tail of the $I-V$ characteristic of such a probe with accuracy of 10%–20% by applying Eq. (17).[84]

The general recipes, however, are not always easily applied for particular conditions. Here we would like to mention a few difficulties, which might arise when a model for probe current is used for given device and plasma parameters. As an illustration we consider a magnetized plasma in the collisional regime. As discussed above, in this case, the collection length (the flux tube where particles are collected from) is much longer than the probe size. In linear machines or in the scrape-off-layer of fusion machines the flux tube terminates on the vessel wall or other structures. Not taking this into account gives rise to underestimated density. If the collection length is known, for example, if it is determined by the machine size, it is possible to modify the probe model.[215,216]

Another problem might be connected with the theoretical assumptions. For instance, in nonlocal or diffusive[75] models for magnetized plasma, the background flows are neglected. To verify the validity of such an assumption, experimental tests or crude estimates can be done. For example, the influence of the $\mathbf{E}\times\mathbf{B}$ background flow can be examined the following way. The known background E field should be compared with electric field due to the probe. The latter field can be estimated to be of the order T_e/eR when the probe collects ion saturation current. This field is normally much larger than the background field for a small perpendicular probe size R. In general, rotation of a perpendicular oriented probe with respect to the flow direction would show variation in the saturation current if the external flow yields a significant contribution to the particle flux into the the flux tube disturbed by the probe.[10] The flow might be important under certain conditions, for instance in space or fast streaming plasmas, or for large probes. A number of theories have been developed for such conditions.[10,24]

The influence of anomalous transport is typical for the application of probes in magnetized plasma. The discussion of the appropriate choice of diffusion and other (for instance, ion mobility) transport coefficients for fusion plasmas can be found in.[16,80] Sometimes, the diffusion coefficient near the probe can be examined experimentally. In Refs. 215, 217, and 218, investigations of this type have been carried out in low-temperature magnetized plasma.

D. Plasma potential

First we discuss how to obtain the plasma potential from the characteristic of the single probe considering the differences that arise in three regimes of probe operation.

In the *collisionless regime*, when the application of the Langmuir formula is valid, various methods have been proposed.[5] The simplest approach is to take the point where the semilog plot of the electron current starts to deviate from a linear function. Another is to take the first or second derivative of the current, since they are more sensitive to current changes. In the ideal case, if I_e depends exponentially on V, and then changes its behavior sharply after passing the plasma potential, the maxima of I_e' and I_e'', and the point where the latter changes sign, should coincide at the plasma potential corresponding to $V=0$ in Fig. 25. In practice, however, the ''knee'' of the characteristic is not that clear and the

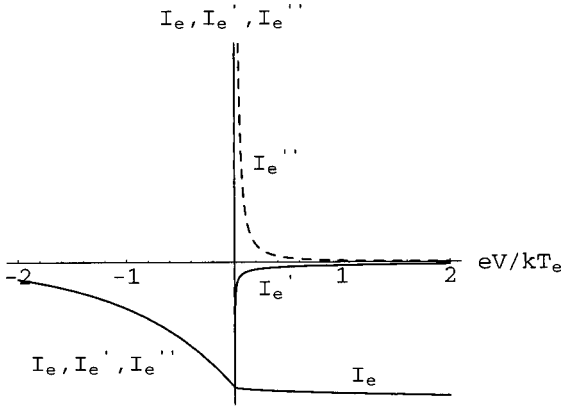

FIG. 25. Electron current I_e (given by Langmuir formula) for repulsive potentials and proportional to $\sqrt{V}$ for attracted potentials, I_e' and I_e'' are first and second derivative of the electron current, respectively. Plasma potential corresponds to $V=0$.

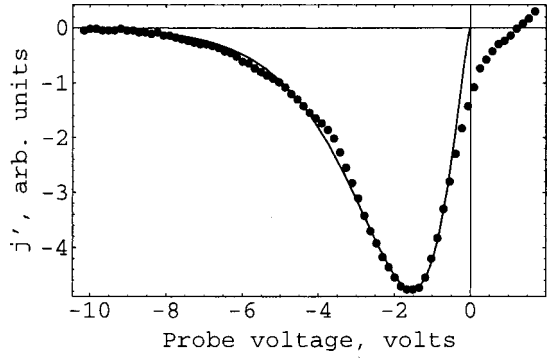

FIG. 27. Measured j' (dots) and fitted theoretical curve (full line) obtained from Eq. (39) for a Maxvellian distribution. Plasma parameters are helium pressure $p=0.3$ Pa, $n=10^{17}$ m^3, and $B=0.15$ T. Measurements have been conducted in a simple magnetized torus Ref. 35 by perpendicular to magnetic field probe with $L=5$ and $R=0.125$ mm. Plasma potential corresponds to $V=0$.

mentioned points do not coincide. This is due to a number of nonideal effects, such as loss of validity of the Langmuir as $V\rightarrow 0$, finite resistivity of plasma, broadening of measured I_e'', fluctuations of plasma potential, etc.[17] In this case, as recommended in Godyak's review,[17] it is advisable to use the zero of the second derivative as the plasma potential.

In the *nonlocal regime*, Eq (36) for unmagnetized and Eqs. (38) and (39) for magnetized plasma show that the first derivative is zero at the plasma potential, while its maximum is shifted from the latter by up to $2T_e/e$ (see Fig. 26 for the magnetized case). In practice, however, to take the point where $I_e'=0$ as the plasma potential is not very reliable due to violation of the validity of the nonlocal model for $V\rightarrow 0$ Ref. 70 and various distortion effects on the measured I_e' (see Sec. II C). Thus, it is advisable to apply the model only for probe potentials in the range $V<-T_e/e$. The plasma potential can be found then by fitting the theoretical curves obtained from Eqs. (36), (38), and (39), for example, for a Maxwellian distribution to the experimental I_e' in this range.[35] The plasma potential corresponds the point where the fitted theoretical curve crosses the zero line, see the example in Fig. 27.

Diffusive models for the *hydrodynamic regime* give similar results. Figure 26 presents the first derivative of the diffusive model for a magnetized plasma.[16] We can see that

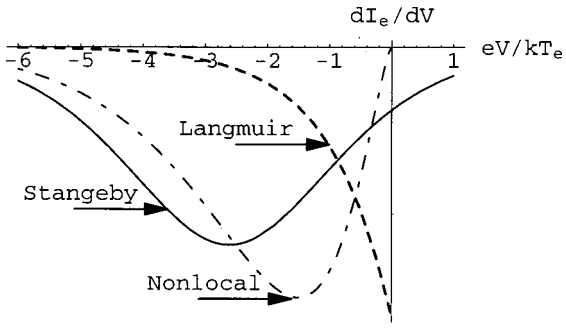

FIG. 26. First derivative of the electron current given by Langmuir formula and diffusive [nonlocal (Eq. 37), Stangeby Refs. 16 and 78)] models. All curves are calculated for the same plasma parameters with classical transport coefficients. Plasma potential corresponds to $V=0$.

the maximum in $|dI_e/dV|$ is shifted with respect to the plasma potential and with respect to the nonlocal model as well. Again, to find the plasma potential, a fitting of appropriate formulas to the experimental curve can be useful.

In order to resolve the fluctuations of the plasma potential, the fast sweep method described earlier can be applied. If the sweep range is large enough to include the transition part of the characteristic, the methods described above are relevant.

Sometimes, it is not possible (hot plasmas) or not practical to sweep the probe potential into the electron saturation region, and thus the sweep is limited to a small range near the floating potential. In this case the indirect method of measuring the plasma potential, based on Eq. (61), has been applied. To recover the V_p fluctuations from that equation one needs measurements of the V_f fluctuations (easily done with any probe), independent measurements of the T_e fluctuations (fast sweep method;[185] triple probe method[219]) and estimates of the coefficient μ. The latter can be problematic since it requires assumptions not only about the electron current but also about the ion current models.

Decreasing the ratio $I_e^{\mathrm{sat}}/I_i^{\mathrm{sat}}$ allows a shift of V_f towards V_p. By methods described below it is possible to achieve a situation when V_f is close to V_p and provides a direct measurement of the instantaneous plasma potential.

One such method is the *emissive probe* technique.[6,15,220–222] The technique employs a probe heated to sufficient temperature to emit thermoelectrons. For probe potentials below V_p a substantial emission current flowing from the probe to the plasma appears as an effective ion current. The potential distribution between probe and plasma depends on the strength of emission. A sufficient amount of electrons residing in front of the probe surface leads to zero electric field near the probe and to space-charge limited current.[6] Figure 28 represents the ideal emission current (dotted lines) and the same with the space-charge effect taken into account (full lines marked as $I_{\mathrm{em}}^{(1)}$ and $I_{\mathrm{em}}^{(2)}$). For the calculation of emission current, formulas provided in Ref. 223 have been used. The curves $I_{\mathrm{em}}^{(1)}$ and $I_{\mathrm{em}}^{(2)}$ correspond to the emission current with probe temperature $T_1=2400$ and $T_2=2500$ K, respectively. Following Ref. 223, the collected

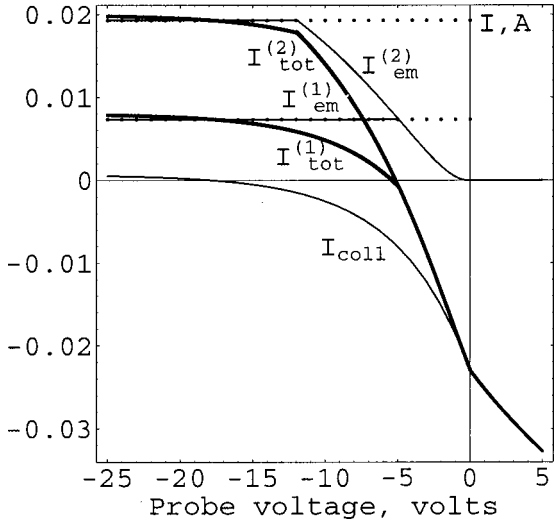

FIG. 28. $I^{(1)}_{em}$ and $I^{(2)}_{em}$ are emission currents calculated with space-charge effect taken into account, corresponding to probe temperature $T_1=2400$ and $T_2=2500$ K, respectively. Electron temperature is $T_e=5$ eV. Dotted lines are ideal emission currents. I_{coll} is probe collection current, $I_{coll}=I_e+I_i$. $I^{(1)}_{tot}$ and $I^{(2)}_{tot}$ are the total currents ($I_{tot}=I_{em}+I_{coll}$) for the emission currents $I^{(1)}_{em}$ and $I^{(2)}_{em}$, respectively. $V=0$ corresponds to the plasma potential.

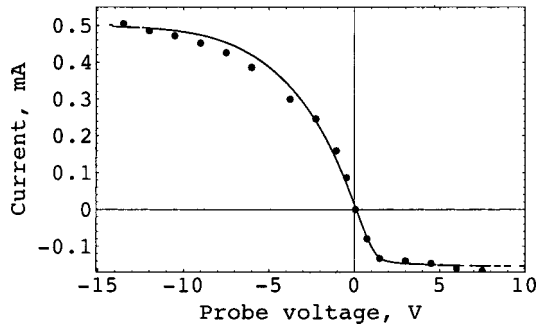

FIG. 29. Plug probe characteristic calculated by application of Eq. (15)–(19) (full curve) and measured (dotted curve). Plasma potential corresponds to $V=0$. The plasma conditions are $B=0.154$ T, helium pressure $p=0.35$ Pa, $n=2\times10^{17}$ m^{-3}, $T_e=2.45$ eV, and $T_i=0.22$ eV. $R=0.25$ mm and $L=18$ mm. In the calculations the theoretical value of I_e was reduced six times to fit the experimental one. After Ref. 227.

current is calculated for the collisionless regime as a sum of the ion current (given by random flux with ion acoustic velocity) and electron current (given by the Langmuir formula). The bold curves named $I^{(1)}_{tot}$ and $I^{(2)}_{tot}$ show measured characteristics of the emissive probe, i.e., sum of the emissive ($I^{(1)}_{em}$ and $I^{(2)}_{em}$, respectively) and collected currents. It is seen that due to space-charge effects the current near the plasma potential is limited, and any further probe heating will not move V_f closer to V_p than $V_p-V_f\sim T_e/e$. Thus, the so-called floating potential technique,[224,225] based on determining the plasma potential by means of the floating potential, gives rise to an error of the order of T_e/e.[223]

Other techniques are the inflection point method[226] and the differential emissive probe.[215,220] The former is based on following the inflection point of the characteristic as the emission is varied to the point of zero emission. The inflection point is determined by taking the derivative of the current. In Ref. 220 a circuit was suggested to control the bias voltage of two emissive probes, which are connected to a differential amplifier. The probe is based on an idea by Chen[6] that the emitting characteristic tends to diverge from the collecting characteristic near the plasma potential. Analytical calculations of the plasma potential by emissive probes and estimates of errors introduced by space-charge effects have been carried out in Ref. 223. A description of secondary emission capacitive probes and self-emissive probes can be found in a Hershkowitz's review.[15]

Application of *ion sensitive probes* operated in the regime where $I_e^{sat}<I_i^{sat}$ (see Sec. IV B) can also provide measurement of the shift of the floating potential. We shall consider here the plug probe as an illustration, as it has been applied for this purpose. The simple geometry of the plug probe permits modeling of this probe by means of theories developed for cylindrical probes in magnetized plasma.[227] Figure 29 presents a theoretical plug probe characteristic (full curve) compared to the experimental one (dots). For this calculation the diffusive model by Rozhanskii[75] was applied [Eqs. (15)–(19)]. In the computations, the effect of the end plugs on the electron current was taken into account by reducing this current by a certain factor to fit the theoretical curve to the experimental one. It is seen from the figure that floating potential of the plug probe is very close to the plasma potential corresponding to $V=0$. The good agreement between the experimental and theoretical curve supports the assumption that the effects of the end plugs is simply to reduce the electron current by a constant factor compared to the unplugged probe. In Ref. 227 it was demonstrated that with this model for the probe current, the fluctuations in V_f due to T_e fluctuations were reduced by almost one order of magnitude compared to the conventional probe and that $\mu\approx0.4$ for the plug probe. A comparison of measurements of time averaged plasma potential by plug and emissive probes demonstrates agreement between two methods within an accuracy of T_e/e.[228] Analysis of a conventional probe characteristic described in the beginning of Sec. IV D yields V_p, which also agrees with V_f of the plug probe within the accuracy of T_e/e.[227] Plug probes are simple to construct and can easily be operated in densely packed probe clusters. The most severe practical difficulty is that the probe requires quite accurate alignment along the magnetic field, which requires accurate alignment of all probes within a cluster. Inside the plasma, optimal alignment is obtained by rotating the probe until minimum electron saturation current is achieved.

E. Electric field

Information about the plasma potential in at least two spatially separated points is necessary to measure the electric field component in the direction of the separation vector between the probes. The smallest E wavelength, λ_{fl} resolved is limited by the half-distance between the probes, i.e., $\lambda_{fl}\geqslant\Delta r/2$. The characteristic scale of the field must be much larger than Δr. On the other hand, the difference between the probe signals becomes weaker as the distance between the probes is reduced, leading to an increase in measurement errors. Such errors include the influence of the probes on

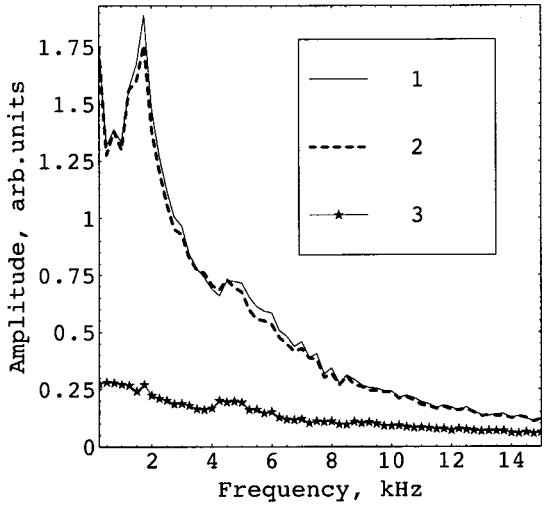

FIG. 30. Amplitude spectra of the plasma potential [curves (1) and (2)] and electric field [curve (3)] measured by two plug probes. The plasma conditions are: $B=0.154$ T, helium pressure $p=0.35$ Pa, $n=2\times10^{17}$ m^{-3}, and $T_e=1$ eV. After Ref. 227.

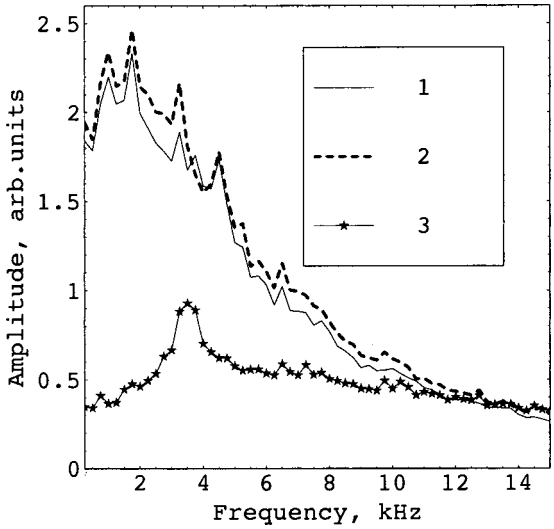

FIG. 31. Amplitude spectra of the plasma potential [curves (1) and (2)] and electric field [curve (3)] measured by two conventional perpendicular floating probes. The plasma conditions are $B=0.154$ T, Helium pressure $p=0.35$ Pa, $n=2\times10^{17}$ m^{-3}, and $T_e=1$ eV. After Ref. 227.

each other and a reduced signal to noise ratio. Therefore, the probe separation has to be chosen as a compromise between the accuracy of measurements and the resolution of the important wavelengths. Since the electric field is obtained as a small difference between two potential signals, the relative errors in the field measurements are usually larger than those of potential measurements.

According to Sec. IV D, in principle, a cluster of two emissive, two plug probes, two fast sweep probes, or a triple probe with two floating pins can be applied. The first three methods yield the plasma potential within the accuracy discussed in Sec. IV D. The last method permits the correction of the floating potential by electron temperature but requires knowledge about μ.

In practice due to their simplicity, two floating conventional probes are often applied under the assumption of small temperature fluctuations. However, as mentioned in Sec. IV D, even small temperature fluctuations can influence the phase of the measured signal and destroy the flux measurements (see Sec. V B). One should remember also that $\tilde{T}_e$ adds with the multiplication factor μ to $\tilde{V}_f$ [see Eq. (61)]. Experimental results from Ref. 227 presented in Figs. 30 and 31 demonstrate errors in E field measurements due to the influence of T_e.

In Figs. 30 and 31 curves (1) and (2) are amplitude spectra of V_p measured at two points by using the floating potential of plug probes (Fig. 30) and of the conventional probe (Fig. 31). According to the discussion in Sec. IV D, the first method yields the plasma potential with an accuracy of $0.4T_e$ while the second method yields a contribution from the electron temperature of μT_e, where $\mu=4.6$ for the given plasma conditions and probe sizes. It is seen from the figures that the contribution of $\tilde{T}_e$ is frequency dependent. For example, at frequency 4 kHz where $\tilde{T}_e\sim0.2\tilde{V}_p$, the amplitude of $\tilde{V}_f$ measured by a conventional probe is twice higher than that measured by a plug probe. The amplitude of E measured by the conventional probes by substituting their floating potentials for the plasma potential [Fig. 31, curve (3)] is four times higher than that measured by the plug probes [Fig. 30, curve (3)]. The difference in floating potential amplitude for the two probe types is not large enough to explain this difference in measured E. There also must be a higher wave number $k(\omega)$ for the signal measured by the conventional probe. As discussed further in Sec. V B, this may indicate that the potential and temperature fluctuations are dominated by two different wave modes with different phase velocity. Obviously, in this case results obtained by conventional probes will lead to significant errors in the measurements of the electric field, and hence (as elaborated in Sec. V B) in the anomalous fluxes.

F. Flow velocity

The influence of plasma flow is particularly important on probe measurements in ionospheric plasma. However, such measurements are beyond the scope of this review and are well documented in the literature.[229–231]

In low pressure (weak magnetic field) laboratory plasma measurements of the anisotropic distribution functions can provide estimates of the flow velocity of electrons. From formulas provided in Sec. III A 2 one can, in principle, recover the directed part of the EDF, $\mathbf{f_1}$ and thus the electron flow velocity. However, the method is cumbersome, and not used much in practice.

In magnetized plasma, measurements of $\mathbf{E}\times\mathbf{B}$ flow, $\mathbf{v}_E=\mathbf{E}\times\mathbf{B}/B^2$, can be conducted by measuring the electric field. Methods for electric field measurements were described in Sec. IV E.

Ion flow parallel to the magnetic field can be measured by means of a *Mach* probe,[19] sometimes also called a *Janus* probe. A sketch of the probe is presented in Fig. 32. Two electrodes are separated by an insulating plate, allowing each of them to detect an ion flux from only one direction. The measured ratio of the ion fluxes (ion saturation current ratio) yields the Mach number. Ion collection by such a probe is

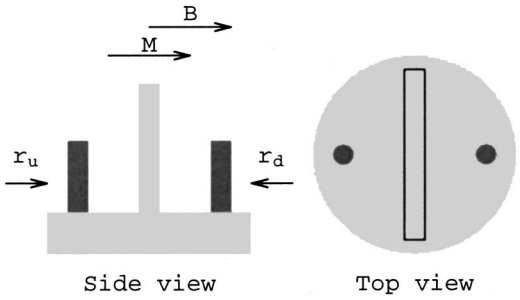

FIG. 32. Sketch of Mach probe. r_u and r_d are upstream and downstream ion fluxes, respectively.

described by fluid models in Refs. 83, 232 and by kinetic models in Ref. 201. More details on the Mach probe can be found in Matthew's review.[19]

V. APPLICATIONS

We have selected two groups of applications, making use of many of the methods discussed in Secs. III and IV. In order to illustrate the usefulness of obtaining the electron energy distribution functions, we discuss some aspects of how this information can be used to gain knowledge about elastic electron collision processes and the inelastic processes involving electrons and atoms/molecules. Furthermore, we illustrate how probe measurements of plasma fluctuations can provide important and detailed information on plasma turbulence, coherent structures, and anomalous fluxes.

A. Plasma electron spectroscopy

As was mentioned in Sec. III, the accuracy of relative measurements of the EDF may be a few percent and that of absolute measurements may be 10%–15%. Therefore, such measurements can be used for quantitative analysis of processes, which are responsible for formation of the EDF. The method of plasma electron spectroscopy is based on measurements of distribution functions for conditions where a part of the distribution function is determined by a particular collision process.[233] In this case, some information about such a process can be extracted. The realization of this idea is simple in an afterglow plasma in which the EDF consists of two groups of electrons. Slow electrons have a Maxwellian with a temperature of order 0.1 eV. The distribution of energetic electrons is far from equilibrium and exhibits a few peaks. These electrons have a density 10^5-10^7 times less than that of slow electrons and appear in reactions like[234]

$$\begin{aligned} &A^*+A^*\rightarrow A^++A+e,\\ &A^*+A^*\rightarrow A_2^++e,\\ &A^*+e\rightarrow A+e, \end{aligned} \tag{64}$$

where A^* denotes an atom in an exited state.

If the diffusion time of the energetic electrons to the boundary is much less than their energy relaxation time in the plasma volume, two types of afterglow can exist.[235,236] When the flux of energetic electrons to the wall is less than the ambipolar flux of ions, so that the electron motion to the wall is a free diffusion, it is simple to create conditions where the EDF of energetic electrons reproduces the electron spectrum of the reactions given by Eq. (64). That makes it possible to investigate the spectrum and the rate constant of these reactions (see, for instance, Fig. 7). The main results of such measurements are summarized in Ref. 126. For the same conditions in Ref. 233 the reflection coefficients of electrons from plasma boundaries have been measured.

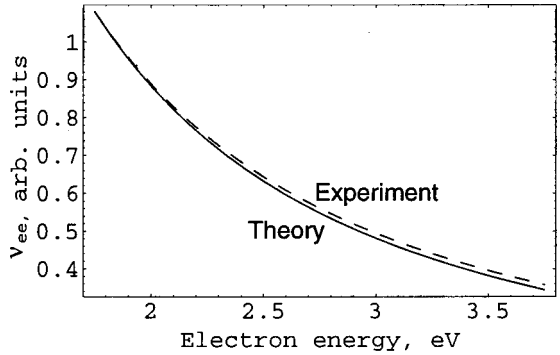

FIG. 33. Electron–electron collisional frequency ν_{ee} as a function of electron energy ε. Theoretical curve is given by Eq. (3). After Ref. 234.

The second type of afterglow occurs when the flux of energetic electrons is greater than the ambipolar flux of ions and, hence, a part of the electrons is captured in the plasma volume, causing continuous spectra of the EDF.[235,236] The continuous spectra are due to collisions of the energetic electrons with neutrals and slow electrons. Creating conditions when collisions with only one of the species (either neutrals or slow electrons) are important allows us to measure the frequency of these collisions.

Figure 33 demonstrates the frequency of electron–electron collisions measured by this method.[233] It might be difficult to obtain this type of information by other methods.

Another method to determine rate constants from EDF measurements was proposed in Ref. 237. The method is based on the measurement of the electron–atom collision integral in an anisotropic plasma. It was applied to the plasma of the positive column of an electric discharge in helium. In this work, the collision integrals S_0, S_1, and the transport cross section of the elastic electron–atom collision were measured.

B. Low-frequency turbulence and transport

Since electric probes can provide instantaneous (on time scales much slower than the ion cyclotron period) measurements of fluid observables, they can be used for studying low-frequency plasma turbulence (drift waves, electrostatic flute-modes, Alfven waves). A two-probe technique due to Beall *et al.*[238] can be implemented to obtain frequency wave-number spectra $S(\omega,k)$. This method assumes a well defined dispersion relation $k=k(\omega)$ for the waves, where k is the wave number in the direction along the separation vector between the two probes. This means that the fluctuations can be represented as a superposition of weakly interacting wave modes (weak turbulence) propagating predominately in a given direction. The broadening of the spectrum $S(\omega,k)$, i.e., the width Δk of $S(\omega,k)$ for a given ω, is given by the characteristic rate κ_{nl} of change of the wave amplitudes and

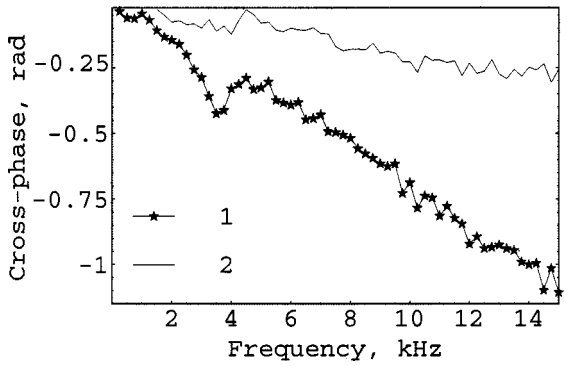

FIG. 34. Phase between two conventional perpendicular (curve 1) and two plug (curve 2) probes. The plasma conditions are $B=0.154$ T, helium pressure $p=0.35$ Pa, $n=2\times10^{17}\,\mathrm{m}^{-3}$, and $T_e=1$ eV. After Ref. 227.

phase due to the nonlinear interaction. If Δk is not small compared to k, the Beall technique has little meaning. A particular outcome of applying this technique is the dispersion relation, which is estimated as follows: assume $g_1(t)$ and $g_2(t)$ are digitized time series of the signals from two probes separated by a vector $\Delta\mathbf{r}$. The *cross power* spectrum of the two signals is defined as $P_{12}(\omega)=\langle G_1^*(\omega)G_2(\omega)\rangle$, where $G_i(\omega)$ is the Fourier transform of $g_i(t)$ and $\langle\cdots\rangle$ denotes an average of a large number of data records. The cross power can be written as $P_{12}=|P_{12}|\exp i\alpha_{12}$, where $\alpha_{12}(\omega)$ is the *cross-phase* spectrum of the signals. If the signals are due to a linear superposition of noninteracting waves,

$$g(\mathbf{r}_i,t)=\int_0^\infty G(\omega)\exp i[\mathbf{k}(\omega)\cdot\mathbf{r}_i-\omega t]d\omega, \tag{65}$$

it is easily shown that $P_{12}(\omega)=\langle|G(\omega)|^2\rangle\exp i[\mathbf{k}(\omega)\cdot\Delta\mathbf{r}]$, and that the *coherence*, $\gamma_{12}(\omega)=|P_{12}(\omega)|/\sqrt{P_{11}(\omega)P_{22}(\omega)}=1$.

Thus, in this case $\alpha_{12}(\omega)=\mathbf{k}(\omega)\cdot\Delta\mathbf{r}$, and the wave-number component $k(\omega)$ along $\Delta\mathbf{r}$ is given by

$$k(\omega)=\alpha_{12}(\omega)/\Delta r. \tag{66}$$

Note that Eq. (65) is far from generally valid, even for noninteracting wave modes. The integral assumes that only one wave vector is excited for every frequency. In general the wave vectors have an angular distribution, and often more than one wave mode is excited. These things create ambiguity with respect to $k(\omega)$, since the definition above may give contributions from wave vectors pointing in different directions and even from several different modes. An example of the latter is shown in Fig. 34, where the cross phase, and hence $k(\omega)$, measured by two conventional probes (curve 1) is four times larger than that measured by plug probes (curve 2). The signal from the conventional probes are dominated by electron temperature fluctuations, while that from plug probes show plasma potential fluctuations. The different wave numbers (and hence propagation velocities) obtained indicate the existence of two different wave modes, one with strong temperature perturbations and another dominated by plasma potential fluctuations.

Some of the quite severe assumptions underlying this technique can be avoided by applying large probe arrays. In the edge of the Caltech tokamak a 32 probe array covered a 7.5 cm poloidal arc in the plasma edge and was used to study the one-dimensional (1D) (poloidal) space-time structure of density fluctuations in edge turbulence.[239] In the same article the two-dimensional (2D) space-time evolution of density and floating potential structures were also studied by means of an 8×8 square probe array (1.8×1.8 cm^2) facing the toroidal magnetic field. In cylindrical magnetized plasmas a circular arrangement of 64 probes has allowed complete azimuthal mapping of fluctuations along the circumference of the plasma column.[240] True space-time results from this array have been compared to results obtained by conditional sampling and averaging of data obtained by the same array in Ref. 241, obtaining quite similar evolution for the large scale structures from the two methods. This gives credibility to the conditional averaging method, which is technically much easier to apply, since it only requires two probes (or probe clusters) and two (or a few) independent channels for digitizing the probe signals. The drawback of this method is that one of the probes must be connected to a computer controlled positioning system.

The conditional averaging method is based on simultaneous sampling of long time series $g_1(\mathbf{r}_1,t)$ from a fixed reference probe at position $\mathbf{r}_1$ and $g_2(\mathbf{r}_1+\Delta\mathbf{r},t)$ from a movable probe, which samples data from a dense grid of positions across the plasma column. The data can either be used to establish a space-time cross-correlation function $C(\Delta\mathbf{r},\tau)=\langle g_1(\mathbf{r}_1,t)g_2(\mathbf{r}_1+\Delta\mathbf{r},t+\tau)\rangle$, or a conditional average $G(\mathbf{r}_2,\tau)=\langle g_2(\mathbf{r}_2,t+\tau)|C_1(t)\rangle$. Here $C_1(t)$ symbolizes a condition imposed on signal g_1 at time t. At those times t_n, $n=1,2,...$, when the condition on $g_1(\mathbf{r}_1,t)$ is met (for instance g_1 exceeds a certain value) the signal $G_n(\mathbf{r}_2,\tau)=g_2(\mathbf{r}_2,t_n+\tau)$ is recorded in a certain window $\tau_{\max}\leqslant\tau\leqslant\tau_{\max}$. The conditional average is then $G(\mathbf{r}_2,\tau)=\lim_{N\to\infty}(1/N)\Sigma_{n=1}^{N}G_n(\mathbf{r}_2,\tau)$. The function $G(\mathbf{r},\tau)$ represents the average space-time evolution of the observable measured by probe 2 in the time window $[-\tau_{\max},\tau_{\max}]$ centered around the time when a conditioning event occurs at the position of probe 1. The method was first introduced in plasma physics in Ref. 242 as a tool to study the evolution of coherent structures, and then applied to Q-machine plasmas as reported in a series of articles.[243–245] It was first applied to toroidal plasmas (the Blaamann device) in Refs. 246, 247, and later to the ADITYA Ref. 248 and TEXT-U Ref. 249 tokamaks.

In Sec. IV we discussed methods for simultaneous measurements of electron density, poloidal electric field, and electron temperature in magnetized plasmas. Such measurements make it possible to obtain the radial, cross-field anomalous flux of particles and energy, and hence to study fundamental properties of anomalous transport relevant for magnetically confined fusion plasmas. In a low-pressure plasma the particle flux density $\Gamma_r=\langle nv_r\rangle=n_0v_{r0}+\langle\tilde{n}\tilde{v}_r\rangle$, is due to convection ($\Gamma_{r0}=n_0v_{r0}$) and electrostatic oscillations in plasma density $\tilde{n}$ and electric field $\tilde{\mathbf{E}}=-\nabla\tilde{\phi}$. The latter gives rise to fluctuations in the plasma drift velocity $v_r\approx E_\theta/B$. By Fourier expansion in time we have

$$\Gamma_r - \Gamma_{r0} = \sum_{\omega>0} \Gamma(\omega) = \frac{2}{B} \sum_{\omega>0} \sqrt{\langle |n(\omega)|^2 \rangle \langle |E_\theta(\omega)|^2 \rangle} \times \gamma_{nE}(\omega) \cos \alpha_{nE}(\omega), \quad (67)$$

where $\gamma_{nE}(\omega) = |\langle n(\omega) E_\theta(\omega)^* \rangle| / \sqrt{\langle |n(\omega)|^2 \rangle \langle |E_\theta(\omega)|^2 \rangle}$ is the cross-coherence and $\alpha_{nE}(\omega) \equiv \arg \langle n(\omega) E_\theta(\omega)^* \rangle$ is the cross-phase between n and E_θ. Assuming a wave superposition such as Eq. (65) we get

$$\Gamma_r - \Gamma_{r0} = \sum_{\omega>0} \Gamma(\omega) = -\frac{2}{B} \sum_{\omega>0} \sqrt{\langle |n(\omega)|^2 \rangle \langle |\phi(\omega)|^2 \rangle} \times k_\theta(\omega) \gamma_{n\phi}(\omega) \sin \alpha_{n\phi}(\omega). \quad (68)$$

These expressions show that the flux is proportional to the power and the cross coherence, and is optimized if $\alpha_{nE} = 0$, $\alpha_{n\phi} = \frac{3}{2}\pi$. The flux is zero if $\alpha_{nE} = \frac{1}{2}\pi$ or $\frac{3}{2}\pi$, $\alpha_{n\phi} = 0$ or π.

If measurements of $n(t)$ and $E_\theta(t)$ are performed simultaneously, the flux density spectrum $\Gamma_r(\omega)$ can be estimated from Eq. (67). Different methods for the E field and n measurements were described in Secs. IV C and IV E. There is a vast literature on flux measurements,[250–252] which means that we can only discuss some illustrative examples. Measurements of E_θ by recording the floating potential on two probe tips separated poloidally were carried out in a Q machine by Nielsen *et al.*[253] The density fluctuations were derived from the ion saturation current. The E field measurements in a reversed field pinch by Ji *et al.*,[219] were performed by means of two floating potentials corrected by T_e fluctuations measured by a triple probe. The problem connected with the determination of μ was discussed in Secs. IV A and IV D. Note, generally, that the method cannot provide the phase correction as the same $\tilde{T}_e$ is subtracted from both floating potentials. A similar approach to E field measurements was used in the Phaedrus-T and TEXT-U tokamaks.[177] In this work, the density fluctuations were obtained from the ion saturation current corrected for T_e fluctuations.

Direct measurements of E allow amplitude and phase errors arising from $\tilde{T}_e$ contribution to be avoided. One example are measurements conducted in a simple magnetized torus by means of a cluster consisting of two plug probes and two conventional probes.[194] In this experiment, $\tilde{E}_\theta$ was measured by plug probes (see Secs. IV D and IV E), $\tilde{T}_e$ by a combination of one plug and one conventional probe (see Sec. IV A) and n_e by application of Eq. (17) for electron saturation current corrected by measurements of $\tilde{T}_e$. Results of these measurements are presented in Fig. 35.

It is also common to obtain $\tilde{E}$ by measuring $\tilde{\phi}$ supplemented by an independent measurement of k_θ using Eq. (66) and signals from two probe tips. Such $\tilde{E}$ measurements combined with a simultaneous measurement of $\tilde{n}$ will then provide the particle flux. This method was first suggested by Powers[254] and has subsequently been applied in a large number of articles. It suffers from possible errors in the measurement of and ambiguities in the very definition of the wave number, k_θ, as described earlier in this subsection.

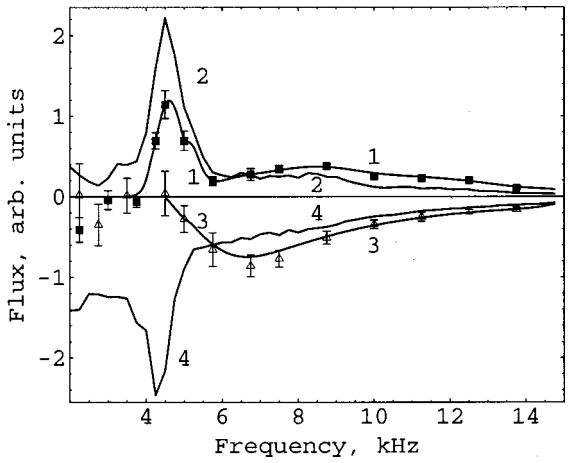

FIG. 35. Particle flux spectrum $\Gamma_r(f)$ [curves (1) and (3)] and heat flux spectrum [curves (2) and (4)] measured by method described in Ref. 194 in simple magnetized torus. The plasma conditions are $B = 0.154$ T, helium pressure $p = 0.35$ Pa, $n = 2 \times 10^{17}$ m^{-3}, and $T_e = 1$ eV.

The cross-field anomalous energy transport is given by[255]

$$Q_r = \frac{3}{2} \Gamma_r T_e + \frac{3}{2} n \frac{\langle \tilde{E}_\theta \tilde{T}_e \rangle}{B}. \quad (69)$$

In many of the works cited above, energy flux is also measured in addition to particle flux. From Eq. (69) it appears that this extension is trivial if $\tilde{T}_e$ is also measured in addition to $\tilde{E}_\theta$ and $\tilde{n}$. Typically, $\tilde{T}_e$ is measured either by the triple probe technique or the fast sweep technique as described in Sec. IV A. For probe measurements on microturbulence and transport in tokamaks more details can be found in the reviews by Hugill[250] and Bretz.[256]

VI. EPILOGUE

From the material presented in this review it should have become clear that electric plasma probes constitute a large arsenal of different diagnostic techniques, some of which are quite ingenious. Still, all techniques are based on the same very simple principle; information about the phase-space distribution of the species of charged particles is extracted from the measured relationship between the current and the voltage applied to one single, or a cluster of small metal objects inserted into the plasma and electrically connected to an external circuit. The focus of this review has been on increasing the awareness of the problems pertaining to the link between the actual plasma conditions, the probe design (e.g., size, geometry, and orientation), and the appropriate theoretical model from which the plasma parameters are inferred from the probe characteristic. If one single message should be extracted from this article, it would be that caution must be exercised in selecting the appropriate probe theory, which is applicable to the plasma conditions and the probe system at hand. Careless application of theoretical models outside their regimes of validity can give rise to gravely incorrect results.

In the present context, the experimentalist is like a practicing physician. The actual plasma is his patient, and the

plasma probe is an invasive diagnostic instrument, which has to be handled with care and caution in order not to upset the patient too much. Plasmas come in a greater variety than human patients, so in this respect the plasma laboratory is more like a veterinary's office. The animal doctor would hardly apply the same diagnostic instrument to a spider and a horse, although the main diagnostic principles would be the same. Thus, the first task of the ''plasma doctor'' is to make a crude examination of the ''patient'' to establish which kind of probes that might be possible to apply in order to acquire the diagnostic information he wants. Once a certain probe design candidate has been found, he has the information required to establish the the probe operation regime according to the classification scheme described in Sec. II. It is important to be aware that, for the same plasma, different probe designs can correspond to different operation regimes, which require different theoretical description. Sometimes this makes it possible to make two or more independent probe measurements of the same plasma observable, which can serve as independent verifications of the methods.

Since this article has focused on the link between plasma conditions, probe design, and probe theory, very little was written about the electric circuitry associated with any probe measurement. This has not been an attempt to downplay the importance of appropriate circuit designs, rather a necessity to limit the length of the review.

ACKNOWLEDGMENTS

The authors are grateful to R. J. Armstrong, M. Koepke, and J. J. Rasmussen for valuable comments. This work was supported by the Research Council of Norway under Grant No. 135373/432.

[1] F. F. Chen, *Introduction to Plasma Physics* (Plenum, New York, 1976).
[2] I. Langmuir and H. M. Mott-Smith, Gen. Electr. Rev. **26**, 731 (1923).
[3] H. M. Mott-Smith and I. Langmuir, Phys. Rev. **28**, 727 (1926).
[4] D. Bohm, E. H. S. Burhop, and H. S. W. Massey, in *Characteristics of Electrical Discharges in Magnetic Fields*, edited by A. Guthrie and R. K. Wakerling (McGraw–Hill, New York, 1949).
[5] Y. M. Kagan and V. I. Perel', Sov. Phys. Usp. **6**, 767 (1964).
[6] F. F. Chen, in *Plasma Diagnostic Techniques*, edited by R. H. Huddlestone and S. L. Leonard (Academic, New York, 1965), p. 113.
[7] L. Schott, in *Plasma Diagnostics*, edited by W. Lohte-Holtgraven (North-Holland, Amsterdam, 1968).
[8] O. V. Kozlov, *An Electrical Probe in a Plasma* (Atomizdat, Moscow, 1969).
[9] J. D. Swift and M. J. R. Schwar, *Electrical Probes for Plasma Diagnostics* (Iliffe Books, London, 1970).
[10] P. L. Chung, L. Talbot, and K. J. Touryan, *Electric Probes in Stationary and Flowing Plasma* (Springer, Berlin, 1975).
[11] Y. A. Ivanov, Y. A. Lebedev, and L. S. Polak, *Methods of In Situ Diagnostics in Non-Equilibrium Plasma-Chemistry* (Nauka, Moscow, 1981).
[12] H. Amemija and Y. Sakamoto, J. Vac. Soc. Jpn. **28**, 177 (1985).
[13] I. H. Hutchinson, *Principles of Plasma Diagnostics* (Cambridge University Press, New York, 1987).
[14] B. V. Alekseev and V. A. Kotel'nikov, *Probe Method for Plasma Diagnostics* (Energoatomizdat, Moscow, 1988).
[15] N. Hershkowitz, in *Plasma Diagnostics* (Academic, Boston, 1989), Vol. 1, p. 113.
[16] P. C. Stangeby, in *Plasma Diagnostics* (Academic, Boston, 1989), Vol. 2, p. 157.
[17] V. A. Godyak, in *Plasma-Surface Interaction and Processing of Materials* (Kluwer, Deventer, 1990), p. 95.
[18] J. E. Allen, Phys. Scr. **45**, 497 (1992).
[19] G. F. Matthews, Plasma Phys. Controlled Fusion **36**, 1595 (1994).
[20] J. E. Allen, Plasma Sources Sci. Technol. **4**, 234 (1995).
[21] V. I. Demidov, N. B. Kolokolov, and A. A. Kudryavtsev, *Probe Methods for Low-Temperature Plasma Investigations* (Energoatomizdat, Moscow, 1996).
[22] M. Tichy, P. Kudrna, J. F. Behnke, C. Csambal, and S. Klagge, J. Phys. IV **7**, 397 (1997).
[23] H. Amemiya, *Diagnostics of Ionized Gas* [The Institute of Physical and Chemical Research (RIKEN), Saitama, 1999].
[24] *Plasma Diagnostics*, edited by A. A. Ovsyannikov and M. F. Zhukov (Cambridge International Science, Cambridge, 2000).
[25] S. Pfau and M. Tichy, in *Low Temperature Plasma Physics. Fundamental Aspects and Applications*, edited by R. Hippler, S. Pfau, M. Schmidt, and K. H. Schoenbach (Wiley, Berlin, 2001).
[26] V. E. Golant, A. P. Zhilinski, and S. A. Sakharov, *Fundamentals of Plasma Physics* (Wiley, New York, 1980).
[27] L. G. H. Huxley and R. W. Crompton, *The Diffusion and Drift of Electrons in Gases* (Wiley, New York, 1974).
[28] E. W. McDaniel, *Collision Phenomena in Ionized Gases* (Wiley, New York, 1964).
[29] D. R. Bates, *Atomic and Molecular Processes* (Academic, New York, 1962).
[30] Y. Itikawa, At. Data Nucl. Data Tables **14**, 2 (1974).
[31] L. M. Biberman, V. S. Vorobev, and I. T. Yakubov, *Kinetics of Nonequilibrium Low-Temperature Plasmas* (Consultants Bureau, New York, 1987).
[32] E. L. Duman and B. M. Smirnov, High Temp. **12**, 431 (1974).
[33] L. D. Tsendin, Sov. J. Plasma Phys. **8**, (1982).
[34] V. I. Kolobov and V. A. Godyak, IEEE Trans. Plasma Sci. **23**, 503 (1995).
[35] V. I. Demidov, S. V. Ratynskaia, R. J. Armstrong, and K. Rypdal, Phys. Plasmas **6**, 350 (1999).
[36] A. V. Phelps, Res. Natl. Inst. Stand. Technol. **95**, 407 (1990).
[37] V. M. Zakharova, Y. M. Kagan, K. S. Mustafin, and V. I. Perel', Sov. Phys. Tech. Phys. **5**, 411 (1960).
[38] C. H. Su and R. E. Kiel, J. Appl. Phys. **37**, 4907 (1966).
[39] I. A. Vasil'eva, High Temp. **12**, 26 (1974).
[40] J. P. Raizer, *Gas Discharge Physics* (Springer, Berlin, 1991).
[41] R. E. Kiel, J. Appl. Phys. **40**, 3668 (1969).
[42] I. P. Shkarofsky, T. W. Johnston, and M. P. Bachinski, *The Particle Kinetics of Plasmas* (Addison-Wesley, London, 1966).
[43] Y. B. Golubovsky, V. M. Zakharova, V. I. Pasunkin, and L. D. Tsendin, Sov. J. Plasma Phys. **7**, 340 (1981).
[44] V. Rozhansky and L. Tsendin, *Transport Phenomena in Partially Ionized Plasma* (Gordon and Breach, New York, 2001).
[45] L. D. Tsendin, Plasma Phys. Sci. Technol. **4**, 200 (1995).
[46] J. R. Sanmartin and R. D. Estes, Phys. Plasmas **6**, 395 (1999).
[47] R. D. Estes and J. R. Sanmartin, Phys. Plasmas **7**, 4320 (2000).
[48] J. E. Allen, R. L. F. Boyd, and P. Reynolds, Proc. Phys. Soc. London, Sect. B **70**, 297 (1957).
[49] I. B. Bernstein and I. N. Rabinowitz, Phys. Fluids **2**, 112 (1959).
[50] F. F. Chen, J. Nucl. Energy, Part C **7**, 47 (1965).
[51] S. H. Lam, Phys. Fluids **8**, 73 (1965).
[52] F. F. Chen, C. Etievant, and D. Mosher, Phys. Fluids **11**, 811 (1968).
[53] J. Virmont and R. Godart, Plasma Phys. **14**, 793 (1972).
[54] I. A. Vasil'eva, High Temp. **12**, 405 (1974).
[55] J. G. Laframboise, Univ. Toronto Inst. Aerospace Rept. 700, 100 (1966).
[56] R. E. Kiel, Agron. J. **6**, 708 (1968).
[57] C. Steinbrüchel, J. Vac. Sci. Technol. A **8**, 1653 (1990).
[58] A. Karamcheti and C. Steinbrüchel, J. Vac. Sci. Technol. A **17**, 3051 (1999).
[59] M. Mausbach, J. Vac. Sci. Technol. A **15**, 2923 (1997).
[60] F. F. Chen, Phys. Plasmas **8**, 3029 (2001).
[61] I. D. Sudit and R. C. Woods, J. Appl. Phys. **76**, 4488 (1994).
[62] M. B. Hopkins and W. G. Graham, Rev. Sci. Instrum. **57**, 2210 (1986).
[63] B. M. Annaratone, M. W. Allen, and J. E. Allen, J. Phys. D **25**, 417 (1992).
[64] M. J. Druyvesteyn, Z. Phys. **64**, 781 (1930).
[65] A. O. McCoubrey, Phys. Rev. **93**, 1249 (1954).
[66] B. Davison, *Neutron Transport Theory* (Oxford University, Oxford, 1958).
[67] J. D. Swift, Proc. Phys. Soc. London **79**, 697 (1962).
[68] M. A. Malkov, High Temp. **29**, 329 (1991).
[69] Y. M. Kagan and V. I. Perel', Sov. Phys. Tech. Phys. **10**, 1445 (1965).
[70] R. R. Arslanbekov, N. A. Khromov, and A. A. Kudryavtsev, Plasma Sources Sci. Technol. **3**, 528 (1994).

[71] V. I. Demidov, S. V. Ratynskaia, and K. Rypdal, Rev. Sci. Instrum. **72**, 4106 (2001).
[72] M. Weinlich and A. Carlson, Phys. Plasmas **4**, 2151 (1997).
[73] V. A. Rozhanskii and A. A. Ushakov, Tech. Phys. Lett. **24**, 869 (1998).
[74] M. Charro and J. R. Sanmartin, Phys. Plasmas **7**, 2622 (2000).
[75] V. A. Rozhanskii and L. D. Tsendin, Sov. Phys. Tech. Phys. **23**, 932 (1978).
[76] V. A. Rozhansky and L. D. Tsendin, *Collisional Transport in a Partly-Ionized Plasma* (Energoatomizdat, Moscow, 1988).
[77] I. M. Cohen, Phys. Fluids **6**, 1492 (1963).
[78] P. C. Stangeby, J. Phys. D **15**, 1007 (1982).
[79] J. R. Sanmartin, Phys. Fluids **13**, 103 (1970).
[80] V. A. Rozhansky, A. A. Ushakov, and S. P. Voskoboynikov, Nucl. Fusion **39**, 613 (1999).
[81] A. Carlson and M. Weinlich, Contrib. Plasma Phys. **38S**, 38 (1998).
[82] R. Chodura, in *Physics of Plasma-Wall Interaction in Controlled Fusion*, edited by D. E. Post and R. Behrisch (Plenum, New York, 1986).
[83] I. H. Hutchinson, Phys. Rev. A **37**, 4358 (1988).
[84] S. V. Ratynskaia, V. I. Demidov, and K. Rypdal, Rev. Sci. Instrum. **71**, 3382 (2000).
[85] V. A. Rozhanskii and L. D. Tsendin, Sov. J. Plasma Phys. **4**, 218 (1978).
[86] A. G. Breslin and K. G. Emeleus, Int. J. Electron. **42**, 433 (1977).
[87] K. G. Emeleus, Int. J. Electron. **47**, 97 (1979).
[88] H. Amemia and G. Fuchs, Jpn. J. Appl. Phys., Part 1 **30**, 3531 (1991).
[89] G. Fuchs, B. Schlarbaum, H. Beuscher, H. G. Mathews, and W. Kraus-Vogt, J. Nucl. Mater. **145-147**, 268 (1987).
[90] V. I. Demidov, Int. J. Electron. **54**, 183 (1983).
[91] V. I. Demidov, N. B. Kolokolov, and O. G. Toronov, Sov. Phys. Tech. Phys. **29**, 230 (1984).
[92] B. C. Bell and D. A. Glocker, J. Vac. Sci. Technol. A **6**, 2047 (1988).
[93] W. E. Amatucci, M. E. Koepke, T. E. Sheridan, M. J. Alport, and J. J. Caroll III, Rev. Sci. Instrum. **64**, 1253 (1993).
[94] D. Strele, M. Koepke, R. Schrittwieser, and P. Winkler, Rev. Sci. Instrum. **68**, 3751 (1997).
[95] G. Medicus, 5th International Conference on Ionization Phenomena in Gases, 1961, Vol. 2, p. 1397.
[96] E. Berger and A. Heisen, J. Phys. D **8**, 629 (1975).
[97] A. Garscadden and K. G. Emeleus, Proc. Phys. Sov. **79**, 535 (1962).
[98] F. W. Crawford, J. Appl. Phys. **34**, 1897 (1963).
[99] A. Boschi and F. Magistrelli, Nuovo Cimento **29**, 487 (1963).
[100] V. A. Godyak, *Soviet Radio Frequency Discharge Research* (Delphic Association, Falls Church, 1986).
[101] K. Matsumoto and M. Sato, J. Appl. Phys. **54**, 1781 (1983).
[102] A. B. Blagoev, V. I. Demidov, N. B. Kolokolov, and O. G. Toronov, Sov. Phys. Tech. Phys. **26**, 1179 (1981).
[103] S. W. Rayment and N. D. Twiddy, Br. J. Appl. Phys., J. Phys. D **2**, 1747 (1969).
[104] S. S. Gulidov, Y. M. Kagan, N. B. Kolokolov, and V. M. Milenin, Sov. Phys. Tech. Phys. **14**, 993 (1969).
[105] V. G. Belov, V. M. Milenin, and N. A. Timofeev, Sov. Phys. Tech. Phys. **28**, 95 (1983).
[106] V. A. Godyak, R. B. Piejak, and B. M. Alexandrovich, Plasma Sources Sci. Technol. **1**, 36 (1992).
[107] I. D. Sudit and F. F. Chen, Plasma Sources Sci. Technol. **3**, 162 (1994).
[108] V. A. Dovzhenko, A. P. Ershov, and G. S. Solntsev, Sov. Phys. Tech. Phys. **19**, 538 (1974).
[109] V. A. Dovzhenko, A. P. Ershov, and G. S. Solntsev, Vestn. MGU, ser. fiz., astron. **19**, 9 (1978).
[110] V. I. Demidov, in *Mathematics with Vision*, edited by V. Keranen and P. Mitic (Computation Mechanics, Southampton, 1995).
[111] K. D. Asvadurov and I. A. Vasil'eva, Sov. Phys. Tech. Phys. **20**, 996 (1975).
[112] K. Wiesemann, Ann. Phys. (Berlin) **27**, 303 (1971).
[113] K. F. Shoenberg, Rev. Sci. Instrum. **51**, 1159 (1980).
[114] H. Amemiya, Trans. Inst. Electr. Eng. Jpn. **103**, 15 (1983).
[115] L. M. Volkova, V. I. Demidov, N. B. Kolokolov, and E. M. Kral'kina, Sov. Phys. Tech. Phys. **28**, 583 (1983).
[116] L. M. Volkova, V. I. Demidov, N. B. Kolokolov, and E. M. Kral'kina, High Temp. **22**, 612 (1984).
[117] V. I. Demidov and N. B. Kolokolov, Sov. Phys. Tech. Phys. **26**, 533 (1981).
[118] H. Amemiya, Jpn. J. Appl. Phys. **15**, 1767 (1976).
[119] T. I. Cox, V. G. I. Deshmukh, D. A. O. Hope, A. J. Hydes, N. S. Braithwaite, and N. M. P. Benjamin, J. Phys. D **20**, 820 (1987).
[120] N. K. Bibinov, D. B. Kokh, N. B. Kolokolov, V. A. Kostenko, D. Meyer, I. P. Vinogradov, and K. Wiesemann, Plasma Sources Sci. Technol. **7**, 298 (1998).
[121] I. P. Vinogradov, Plasma Sources Sci. Technol. **8**, 299 (1999).
[122] H. Sugai, H. Toyoda, K. Nakano, and N. Isomura, Plasma Sources Sci. Technol. **4**, 366 (1995).
[123] R. L. Stenzel, W. Gekelman, N. Wild, J. M. Urrutia, and D. Whelan, Rev. Sci. Instrum. **54**, 1302 (1983).
[124] *Electron Kinetics and Applications of Glow Discharges*, edited by U. Kortshagen and L. D. Tsendin, NATO ASI Series B Physics (NATO, City, 1998), p. 367.
[125] N. B. Kolokolov, A. A. Kudrjavtsev, and A. B. Blagoev, Phys. Scr. **50**, 371 (1994).
[126] N. B. Kolokolov and A. B. Blagoev, Sov. Phys. Usp. **163**, 55 (1993).
[127] N. A. Gorbunov, N. B. Kolokolov, and A. A. Kudryavtsev, Sov. J. Plasma Phys. **15**, 881 (1989).
[128] N. A. Gorbunov, N. B. Kolokolov, and F. E. Latyshev, Tech. Phys. **46**, 391 (2001).
[129] A. Y. Popov (private communication, 2001).
[130] F. M. Morse and G. Feshbach, *Methods of Theoretical Physics*, Part 1 (McGraw-Hill, New York, 1980).
[131] P. J. Chantry, J. Appl. Phys. **62**, 1141 (1987).
[132] C. J. Howard, J. Phys. Chem. **83**, 3 (1979).
[133] Y. M. Kagan and V. I. Perel', Sov. Phys. Tech. Phys. **13**, 141 (1968).
[134] V. L. Fedorov, Sov. Phys. Tech. Phys. **30**, 584 (1985).
[135] R. C. Woods and I. D. Sudit, Phys. Rev. **50**, 2222 (1994).
[136] G. Korn and T. Korn, *Mathematical Handbook for Scientists and Engineers* (McGraw-Hill New York, 1968).
[137] V. F. Lapshin and A. S. Mustafaev, Sov. Phys. Tech. Phys. **34**, 150 (1989).
[138] A. P. Mezentsev, A. S. Mustafaev, and V. L. Fedorov, J. Phys. D **21**, 1464 (1988).
[139] V. F. Lapshin, A. P. Mezentsev, and A. S. Mustafaev, J. Phys. D **22**, 857 (1989).
[140] F. G. Baksht, V. F. Lapshin, and A. S. Mustafaev, J. Phys. D **28**, 689 (1995).
[141] V. I. Demidov, N. B. Kolokolov, A. S. Mezentsev, and A. S. Mustafaev, Sov. J. Plasma Phys. **12**, 866 (1986).
[142] A. S. Mustafaev, Tech. Phys. **46**, 472 (2001).
[143] S. Klagge and A. Lunk, J. Appl. Phys. **70**, 99 (1991).
[144] E. Passoth *et al.*, J. Phys. D **32**, 2655 (1999).
[145] V. I. Demidov, in *Innovation in Mathematics*, edited by V. Keranen and P. Mitic (Computational Mechanics, Southampton, 1997).
[146] Y. M. Kagan, B. P. Lavrov, and R. I. Lyaguschenko, Sov. Phys. Tech. Phys. **22**, 349 (1977).
[147] M. A. Abroyan, V. I. Demidov, Y. M. Kagan, N. B. Kolokolov, and B. P. Lavrov, Opt. Spectrosc. **39**, 13 (1975).
[148] H. Amemija, J. Phys. Soc. Jpn. **57**, 887 (1988).
[149] H. Amemija, J. Phys. D **23**, 999 (1990).
[150] E. Bogdanov, A. A. Kudryavtsev, and V. N. Skrebov, Bull. Russ. Akad. Sci. Phys. **63**, 1730 (1999).
[151] S. M. Fereira, G. Gousset, and M. Touzeau, J. Phys. D **21**, 1403 (1988).
[152] S. A. Gutsev, A. A. Kudryavtsev, and V. A. Romanenko, Tech. Phys. **40**, 1131 (1995).
[153] S. A. Gutsev, N. A. Khromov, A. A. Kudryavtsev, and V. A. Romanenko, *Proceedings of the Eleventh International Conference on Gas Discharges and their Applications* (Institute of Electrical Engineering, Japan, Tokyo, 1995), Vol. 2, p. 108.
[154] H. Amemiya, Jpn. J. Appl. Phys., Part 1 **27**, 1966 (1988).
[155] I. Katsumata and M. Okazaki, Jpn. J. Appl. Phys. **6**, 123 (1967).
[156] M. Sato, Phys. Fluids **17**, 1903 (1974).
[157] V. I. Demidov, S. V. Ratynskaia, and K. Rypdal, Rev. Sci. Instrum. **70**, 4266 (1999).
[158] S. V. Ratynskaia, V. I. Demidov, and K. Rypdal, Rev. Sci. Instrum. (accepted).
[159] J. I. F. Palop, J. Ballesteros, V. Colomer, and M. A. Hernandez, Rev. Sci. Instrum. **66**, 4625 (1995).
[160] F. M. Dias and E. Tatarova, J. Phys. IV **8**, 257 (1998).
[161] R. Sloan and McGregor, Philos. Mag. A **18**, 193 (1934).
[162] G. A. Branner, E. M. Friar, and G. Medicus, Rev. Sci. Instrum. **34**, 231 (1963).
[163] G. M. Malishev and V. L. Fedorov, DAN SSSR **93**, 269 (1953).
[164] F. M. Dias, Plasma Sources Sci. Technol. **4**, 86 (1995).
[165] K. Shimizu and H. Amemiya, J. Phys. E **9**, 943 (1976).
[166] B. V. Kuteev and V. A. Rozhanskii, Sov. Tech. Phys. Lett. **4**, 49 (1978).

[167] B. V. Kuteev, V. A. Rozhanskii, and L. D. Tsendin, Beitr. Plasmaphys. **19**, 123 (1979).
[168] E. O. Johnson and L. Malter, Phys. Rev. **80**, 58 (1950).
[169] S. Klagger and M. Tichy, Czech. J. Phys., Sect. B **35**, 988 (1985).
[170] D. C. Robinson and M. G. Rusbridge, Phys. Plasmas **11**, 73 (1969).
[171] H. Lin, R. D. Bengtson, and C. P. Ritz, Phys. Fluids B **1**, 2027 (1989).
[172] H. Lin, G. X. Li, R. D. Bengtson, C. P. Ritz, and H. Y. W. Tsui, Rev. Sci. Instrum. **63**, 4612 (1992).
[173] Sin-Li Chen and T. Sekiguchi, J. Appl. Phys. **36**, 2363 (1965).
[174] M. Kamitsuma, Sin-Li Chen, and Jen-Shih Chang, J. Appl. Phys. **10**, 1065 (1977).
[175] M. Laux, Phys. Plasmas **41**, 510 (2001).
[176] A. Carlson, L. Giannone, and the ASDEX Team, *Proceedings of the EPS, Berlin*, Vol. 15C, Part IV, p. 305, 1991.
[177] H. Y. W. Tsui *et al.*, Rev. Sci. Instrum. **63**, 4608 (1992).
[178] M. A. Meier *et al.*, Rev. Sci. Instrum. **66**, 437 (1995).
[179] M. A. Meier *et al.*, Rev. Sci. Instrum. **68**, 369 (1997).
[180] M. A. Meier, G. A. Hallock, and R. D. Bengtson, Contrib. Plasma Phys. **38S**, 98 (1998).
[181] P. C. Liewer, J. M. McChesney, S. J. Zweben, and R. W. Gould, Phys. Fluids **29**, 309 (1986).
[182] C. Hidalgo, R. Balbin, M. A. Pedrosa, I. Garsia-Cortes, and M. A. Ochando, Phys. Rev. Lett. **69**, 1205 (1992).
[183] R. Balbin, C. Hidalgo, M. A. Pedrosa, and I. Garsia-Cortes, Rev. Sci. Instrum. **63**, 4605 (1992).
[184] L. Giannone *et al.*, Phys. Plasmas **1**, 3614 (1994).
[185] C. Hidalgo *et al.*, Contrib. Plasma Phys. **36S**, 139 (1996).
[186] F. W. Crawford and R. Grand, J. Appl. Phys. **37**, 180 (1966).
[187] A. Nedospasov and D. Uzdensky, Contrib. Plasma Phys. **34**, 478 (1994).
[188] P. Verplancke *et al.*, Contrib. Plasma Phys. **36S**, 145 (1996).
[189] T. F. Yang, Q. X. Zu, and Ping Liu, Rev. Sci. Instrum. **66**, 3879 (1995).
[190] R. Van Nieuwenhove and G. Van Oost, Rev. Sci. Instrum. **59**, 1053 (1988).
[191] L. M. Bogomolov *et al.*, Sov. J. Plasma Phys. **18**, 419 (1992).
[192] J. A. Boedo *et al.*, Rev. Sci. Instrum. **70**, 2997 (1999).
[193] S. V. Ratynskaia, V. I. Demidov, and K. Rypdal, Rev. Sci. Instrum. **71**, 1367 (2000).
[194] S. Ratynskaia, V. Demidov, and K. Rypdal, Phys. Rev. E **65**, 066403 (2002).
[195] G. F. Matthews, J. Phys. D **17**, 2243 (1984).
[196] A. S. Wan, T. F. Yang, B. Lipschultz, and B. LaBombard, Rev. Sci. Instrum. **57**, 1542 (1986).
[197] R. A. Pitts, Phys. Fluids **3**, 2271 (1991).
[198] R. A. Pitts, Contrib. Plasma Phys. **36S**, 87 (1996).
[199] D. L. Rudakov *et al.*, Rev. Sci. Instrum. **70**, 476 (1999).
[200] F. Valsaque, G. Manfredi, J. P. Gunn, and E. Gauthier, Phys. Plasmas **9**, 1806 (2002).
[201] K.-S. Chung and I. H. Hutchinson, Phys. Rev. A **38**, 4721 (1988).
[202] Y. Okuno, Y. Ohtsu, and H. Fujita, J. Appl. Phys. **74**, 5990 (1993).
[203] I. N. Churkin, V. I. Volosov, and A. G. Steshov, Rev. Sci. Instrum. **70**, 3930 (1999).
[204] C. Böhm and J. Perrin, Rev. Sci. Instrum. **64**, 31 (1993).
[205] I. Katsumata, Contrib. Plasma Phys. **36S**, 73 (1996).
[206] A. Bergmann, 20th EPS Conference on Control. Fusion and Plasma Phys. (Lisbon), 1993, Vol. 17C II, p. 803.
[207] N. Ezumi, Contrib. Plasma Phys. **41**, 488 (2001).
[208] M. J. McCarrick, R. F. Ellis, M. Koepke, and R. P. Majeski, Rev. Sci. Instrum. **56**, 1463 (1985).
[209] W. E. Amatucci *et al.*, J. Geophys. Res. **103**, 11 711 (1998).
[210] M. Sato, Phys. Fluids **15**, 2427 (1972).
[211] I. Arikata *et al.*, Jpn. J. Appl. Phys., Part 1 **24**, 512 (1985).
[212] D. M. Manos *et al.*, J. Nucl. Mater. **111-112**, 130 (1982).
[213] P. C. Stangeby *et al.*, J. Vac. Sci. Technol. A **1**, 1302 (1983).
[214] H. Amemiya and U. Ueraha, Rev. Sci. Instrum. **65**, 2607 (1994).
[215] E. Y. Wang *et al.*, Rev. Sci. Instrum. **57**, 2425 (1986).
[216] P. C. Stangeby, *The Plasma Boundary of Magnetic Fusion Devices* (Institute of Physics, London, 2000).
[217] V. Demidov, S. Ratynskaia, and K. Rypdal, Contrib. Plasma Phys. **41**, 443 (2001).
[218] M. Stanojevic *et al.*, Contrib. Plasma Phys. **34**, 241 (1994).
[219] H. Ji, H. Toyama, K. Miyamoto, S. Shinohara, and A. Fujisawa, Phys. Rev. Lett. **67**, 62 (1991).
[220] Wang En Yao, I. Intrator, and N. Hershkowitz, Rev. Sci. Instrum. **56**, 519 (1985).
[221] A. Siebenforcher and R. Schrittwieser, Rev. Sci. Instrum. **67**, 849 (1996).
[222] R. Schrittwieser, C. Ionita, P. C. Balan, J. A. Cabral, F. H. Figueiredo, V. Pohoata, and C. Varandas, Contrib. Plasma Phys. **41**, 494 (2001).
[223] M. Y. Ye and S. Takamura, Phys. Plasmas **7**, 3457 (2000).
[224] R. F. Kemp and J. M. Sellen, Rev. Sci. Instrum. **37**, 455 (1966).
[225] H. Yamada and D. L. Murphee, Phys. Fluids **14**, 1120 (1971).
[226] J. R. Smith, N. Hershkowitz, and P. Coakley, Rev. Sci. Instrum. **50**, 210 (1979).
[227] S. Ratynskaia, V. Demidov, and K. Rypdal, Phys. Plasmas (accepted).
[228] D. Block *et al.*, *Proceedings of the ICPP 2002* (to be published).
[229] J. G. Laframboise and L. J. Sonmor, J. Geophys. Res., [Space Phys.] **98**, 337 (1993).
[230] J. G. Laframboise, J. Geophys. Res., [Space Phys.] **102**, 2417 (1997).
[231] H. Gunell, M. Larsson, and N. Brenning, Geophys. Res. Lett. **27**, 161 (2000).
[232] P. C. Stangeby, Phys. Fluids **27**, 2699 (1984).
[233] V. I. Demidov and N. B. Kolokolov, Sov. Phys. J. **30**, 97 (1987).
[234] P. Monchicourt, M. Touzeau, and W. E. Wells, J. Phys. **34**, C2-145 (1973).
[235] V. I. Demidov and N. B. Kolokolov, Sov. Phys. Tech. Phys. **25**, 338 (1980).
[236] V. I. Demidov and N. B. Kolokolov, Phys. Lett. A **89**, 397 (1982).
[237] A. P. Mezentsev, A. S. Mustafaev, V. F. Lapshin, and V. L. Fedorov, J. Phys. B **20**, L723 (1987).
[238] J. M. Beall, Y. C. Kim, and E. J. Powers, J. Appl. Phys. **53**, 3933 (1982).
[239] S. J. Zweben and R. W. Gould, Nucl. Fusion **25**, 171 (1985).
[240] A. Latten, T. Klinger, A. Piel, and T. Pierre, Rev. Sci. Instrum. **66**, 3254 (1995).
[241] O. Grulke, T. Klinger, and A. Piel, Phys. Plasmas **6**, 788 (1999).
[242] H. Johnsen, H. L. Pécseli, and J. Trulsen, Phys. Fluids **30**, 2239 (1987).
[243] A. H. Nielsen, H. L. Pécseli, and J. J. Rasmussen, Ann. Geophys. **10**, 655 (1992).
[244] H. L. Pécseli, E. A. Coutsias, T. Huld, J. P. Lynov, A. H. Nielsen, and J. J. Rasmussen, Comments Plasma Phys. Controlled Fusion **10**, 2065 (1992).
[245] A. H. Nielsen, H. L. Pécseli, and J. J. Rasmussen, Phys. Scr. **51**, 632 (1994).
[246] F. J. Øynes, H. L. Pécseli, and K. Rypdal, Phys. Rev. Lett. **75**, 81 (1995).
[247] F. J. Øynes, O.-M. Olsen, H. L. Pécseli, Å. Fredriksen, and K. Rypdal, Phys. Rev. E **57**, 2242 (1998).
[248] B. K. Joseph, R. Jha, P. K. Kaw, S. K. Mattoo, C. V. S. Rao, and Y. C. Saxena, Phys. Plasmas **4**, 4292 (1997).
[249] M. S. Foster, J. L. Craig, and A. J. Wooton, Rev. Sci. Instrum. **66**, 461 (1995).
[250] J. Hugill, Plasma Phys. Controlled Fusion **42**, R75 (2000).
[251] P. Mantica, G. Vayakis, J. Hugill, S. Cirant, R. A. Pitts, and G. F. Matthews, Nucl. Fusion **31**, 1649 (1991).
[252] B. LaBombard, Phys. Plasmas **9**, 1300 (2002).
[253] A. H. Nielsen, H. L. Pécseli, and J. J. Rasmussen, Ann. Geophys. **3**, 1530 (1996).
[254] E. J. Powers, Nucl. Fusion **14**, 794 (1974).
[255] D. W. Ross, Comments Plasma Phys. Controlled Fusion **12**, 155 (1989).
[256] N. Bretz, Rev. Sci. Instrum. **68**, 2927 (1997).